

Numerical solution of Q^2 evolution equations in a brute-force method

M. Miyama and S. Kumano *

Department of Physics, Saga University, Saga 840, Japan
and

Physics Department, Brookhaven National Laboratory
Upton, New York, 11973-5000, U.S.A.

ABSTRACT

We investigate numerical solution of Q^2 evolution equations for structure functions in the nucleon and in nuclei. (Dokshitzer-Gribov-Lipatov-)Altarelli-Parisi and Mueller-Qiu evolution equations are solved in a brute-force method. Spin-independent flavor-nonsinglet and singlet equations with next-to-leading-order α_s corrections are studied. Dividing the variables x and Q^2 into small steps, we simply solve the integrodifferential equations. Numerical results indicate that accuracy is better than 2% in the region $10^{-4} < x < 0.8$ if more than two-hundred Q^2 steps and more than one-thousand x steps are taken. The numerical solution is discussed in detail, and evolution results are compared with Q^2 dependent data in CDHSW, SLAC, BCDMS, EMC, NMC, Fermilab-E665, ZEUS, and H1 experiments. We provide a FORTRAN program for Q^2 evolution (and “devolution”) of nonsinglet-quark, singlet-quark, $q_i + \bar{q}_i$, and gluon distributions (and corresponding structure functions) in the nucleon and in nuclei. This is a very useful program for studying spin-independent structure functions.

* Email: 94sm10 or kumanos@cc.saga-u.ac.jp. Information on their research is available at <http://www.cc.saga-u.ac.jp/saga-u/riko/physics/quantum1/structure.html> or at <ftp://ftp.cc.saga-u.ac.jp/pub/paper/riko/quantum1>.

Program Summary

Title of program: BF1

Computer: AlphaServer 2100 4/200; *Installation:* The Research Center for Nuclear Physics in Osaka

Operating system: OpenVMS V6.1

Programming language used: FORTRAN 77

Peripherals used: Laser printer

No. of lines in distributed program, including test data, etc.: 2439

Keywords: Structure function, parton distribution, Q^2 evolution, numerical solution.

Nature of physical problem

This program solves Altarelli-Parisi equations or modified evolution equations (Mueller-Qiu) with or without next-to-leading-order α_s effects for a spin-independent structure function or quark distribution. Both flavor-nonsinglet and singlet cases are provided, so that the distributions, xq_{NS} , xq_S , $xq_i^+ \equiv xq_i + x\bar{q}_i$ (i =quark flavor), xg , xF_{NS} , xF_S , and xF_i^+ in the nucleon and in nuclei can be evolved.

Method of solution

We divide the variable x (and Q^2) into very small steps, and integration and differentiation are defined by $\frac{df(x)}{dx} = \frac{[f(x_{m+1}) - f(x_m)]}{\Delta x_m}$ and $\int dx f(x) = \sum_{m=1}^{N_x} \Delta x_m f(x_m)$.

Then, the integrodifferential equations are simply solved step by step, and this method is so called brute-force method. If the step numbers are increased, accurate results should be obtained.

Restrictions of the program

This program is used for calculating Q^2 evolution of a spin-independent flavor-nonsinglet-quark, singlet-quark, q_i^+ , and gluon distributions (and corresponding structure functions) in the leading order or in the next-to-leading-order of α_s . Q^2 evolution equations are the Altarelli-Parisi equations and the modified ones (Mueller-Qiu). The double precision arithmetic is used. The renormalization scheme is the modified minimal subtraction scheme (\overline{MS}). A user provides the initial structure function or quark distribution as a subroutine or as a data file. Examples are explained in sections 4.2 and 4.3. Then, the user inputs twenty-one parameters in section 4.1.

Typical running time

Approximately five minutes on AlphaServer 2100 4/200 in the nonsinglet case, sixty minutes in the singlet-quark evolution, and eighty minutes in the singlet evolution with recombination effects.

LONG WRITE-UP

1. Introduction

Subnucleon degrees of freedom could be investigated in high-energy lepton-nucleon interactions. Measured structure functions depend in general on two variables, $Q^2 = -q^2$ and $x = Q^2/2P \cdot q$, where q is the four-momentum transfer and P is the nucleon momentum. Bjorken scaling hypothesis suggests that structure functions are independent of Q^2 . However, the scaling is not exactly satisfied and they have weak logarithmic Q^2 dependence, which is referred to as scaling violation. Although the structure functions themselves cannot be calculated except for lattice QCD methods, it is possible to estimate their Q^2 variations within perturbative QCD.

An intuitive way of describing the scaling violation is to use the (Dokshitzer-Gribov-Lipatov-)Altarelli-Parisi equation [1]. For example, the flavor-nonsinglet Altarelli-Parisi (or DGLAP) equation is given by

$$\frac{\partial}{\partial \ln Q^2} q_{NS}(x, Q^2) = \frac{\alpha_s(Q^2)}{2\pi} \int_x^1 \frac{dy}{y} P_{NS}\left(\frac{x}{y}\right) q_{NS}(y, Q^2) \quad , \quad (1.1)$$

where $q_{NS}(x, Q^2)$ is a nonsinglet quark distribution, $P_{NS}(x)$ is a nonsinglet splitting function, and $\alpha_s(Q^2)$ is the running coupling constant. The integrodifferential equation describes the progress that a quark with the nucleon's momentum fraction y radiates a gluon and it becomes a quark with the momentum fraction x . The splitting function determines the probability of the splitting process. The singlet Altarelli-Parisi equations are more complicated due to gluon participation in the evolution process. The flavor-singlet part is given by coupled integrodifferential equations, which are discussed in section 2.

We study not only the Altarelli-Parisi equations but also modified evolution equations due to parton recombinations (Mueller and Qiu) [2]. The recombination mechanism produces additional terms in the Altarelli-Parisi evolution equations. Because gluons play a major role at small x , gluon recombination processes are investigated in Ref. [2]. Although the nonsinglet equation remains unchanged, the singlet equations are modified due to the gluon recombinations. The additional terms are nonlinear, so that it is not obvious how to solve the evolution equation numerically. On the other hand, the parton recombination mechanism is increasingly important due to recent HERA data in the small x region. It is interesting to test whether the F_2 data at small x could be related to higher-twist effects such as the recombination contributions [3]. In addition, the recombination mechanism is used for explaining nuclear shadowing [4], and it is an important factor in Q^2 evolution of nuclear structure functions.

The Q^2 evolution equations are often used in experimental analysis and also in theoretical calculations, so that it is worth while creating a computer program in solving the equations accurately. A number of methods have been developed [5], and they

include brute-force methods, Mellin-transformation methods, and orthogonal polynomial methods. Among these methods, the Laguerre-polynomial one [6] is considered an efficient one in computing time and in numerical accuracy. We have been investigating the Laguerre method and find that accuracy may not be very satisfactory at small x and at large x particularly in the nonsinglet case. With development of high-energy accelerators, the small x region becomes important. In fact, the x region of 10^{-4} could be reached with large enough Q^2 at which perturbative QCD could be used. Considering structure-function studies at HERA and at future high-energy laboratories, we should have a computer program which enables the evolution with good accuracy at small x . In addition to this problem, there is other difficulty in the Laguerre method. It is not obvious how to apply the Laguerre method to the case of modified Q^2 evolution equations with parton recombinations. It is because of the existence of nonlinear recombination terms in the evolution equations.

These issues motivated us to explore an alternative method. As a possible way to solve the above difficulties, we study a brute-force method. This method was, for example, investigated in Ref. [7]; however, there is no published article in discussing the details of the solution and its accuracy. The method is perhaps the simplest one in solving the integrodifferential equations. We divide the variables x and Q^2 into very small steps, and integration and differentiation are defined by $df(x)/dx = [f(x_{m+1}) - f(x_m)]/\Delta x_m$ and $\int dx f(x) = \sum_{m=1}^{N_x} \Delta x_m f(x_m)$. Then, the evolution equation can be solved step by step. If N_x is large enough, we should be able to get accurate numerical results. Our research purposes are to investigate the details of numerical accuracy and to provide a useful computer program in the brute-force method.

The evolution equations, which are solved by the brute-force method, are given in section 2. We explain the brute-force method in section 3. In section 4, information for running the program BF1 is supplied. Each subroutine in the program is explained in section 5. Numerical results and comparisons with experimental data are given in section 6. The results are summarized in section 7. Explicit equations of the splitting functions and other necessary quantities are given in appendices.

2. Q^2 evolution equations

We solve two types of evolution equations. One is the ordinary equations, so called Altarelli and Parisi equations, and the other is the modified ones due to recombinations by Mueller and Qiu. Parton distributions or structure functions in the nucleon can be evolved in both methods. The modified equations can also handle evolution of nuclear parton distributions.

2.1 (Dokshitzer-Gribov-Lipatov-)Altarelli-Parisi equations

The nonsinglet ‘‘Altarelli-Parisi’’ equation is given in Eq. (1.1), which is valid both in the leading order (LO) case and in the next-to-leading order (NLO) one. NLO effects can be included in the running coupling constant $\alpha_s(t)$ and in the splitting functions $P_{ij}(z)$. In order to remove the extra Q^2 dependence in front of the integral in Eq. (1.1), we use the variable t defined by

$$t \equiv -\frac{2}{\beta_0} \ln \left[\frac{\alpha_s(Q^2)}{\alpha_s(Q_0^2)} \right] \quad , \quad (2.1)$$

instead of Q^2 . The parton distribution and the splitting function multiplied by x satisfy the same integrodifferential equation. Therefore, defining $\tilde{f}(x)$ by

$$\tilde{f}(x) = x f(x) \quad , \quad (2.2)$$

we rewrite the evolution equation as

$$\frac{\partial}{\partial t} \tilde{q}_{NS}(x, t) = \int_x^1 \frac{dy}{y} \tilde{P}_{NS}\left(\frac{x}{y}\right) \tilde{q}_{NS}(y, t) \quad . \quad (2.3)$$

The singlet case is more complicated than the nonsinglet one due to the gluon participation in the evolution, and it becomes coupled integrodifferential equations. The singlet quark distribution is defined by $q_s(x, t) = \sum_i q_i^+(x, t)$, where i is the quark flavor and the q_i^+ distribution is given by $q_i^+(x, t) = q_i(x, t) + \bar{q}_i(x, t)$. We write evolution equations in terms of the q_i^+ distribution [8, 9]:

$$\frac{\partial}{\partial t} \tilde{q}_i^+(x, t) = \int_x^1 \frac{dy}{y} \left[\sum_j \tilde{P}_{q_i^+ q_j^+} \left(\frac{x}{y} \right) \tilde{q}_j^+(y, t) + \tilde{P}_{qg} \left(\frac{x}{y} \right) \tilde{g}(y, t) \right] \quad , \quad (2.4a)$$

$$\frac{\partial}{\partial t} \tilde{g}(x, t) = \int_x^1 \frac{dy}{y} \left[\sum_j \tilde{P}_{gq_j^+} \left(\frac{x}{y} \right) \tilde{q}_j^+(y, t) + \tilde{P}_{gg} \left(\frac{x}{y} \right) \tilde{g}(y, t) \right] \quad . \quad (2.4b)$$

Each term in Eqs. (2.4a) and (2.4b) describes the process that a parton p_j with the nucleon’s momentum fraction y splits into a parton p_i with the momentum fraction

x and another parton. The splitting function $P_{p_i p_j}(z)$ determines the probability that such a splitting process occurs and the p_j -parton momentum is reduced by the fraction z . Using $\tilde{P}_{q_i^+ q_j^+}^{(1)}(x) = \delta_{ij} \tilde{P}_{q^+, NS}^{(1)} + 2C_F T_R x F_{qq}(x)$ [8] and $\tilde{P}_{qq^+}(x) =$ (independent of j), we obtain

$$\begin{aligned} \frac{\partial}{\partial t} \tilde{q}_i^+(x, t) = \int_x^1 \frac{dy}{y} \left[\tilde{P}_{q^+, NS} \left(\frac{x}{y} \right) \tilde{q}_i^+(y, t) + 2C_F T_R \tilde{F}_{qq} \left(\frac{x}{y} \right) \tilde{q}_s(y, t) \right. \\ \left. + \tilde{P}_{qg} \left(\frac{x}{y} \right) \tilde{g}(y, t) \right] , \quad (2.5a) \end{aligned}$$

$$\frac{\partial}{\partial t} \tilde{g}(x, t) = \int_x^1 \frac{dy}{y} \left[\tilde{P}_{gq^+} \left(\frac{x}{y} \right) \tilde{q}_s(y, t) + \tilde{P}_{gg} \left(\frac{x}{y} \right) \tilde{g}(y, t) \right] . \quad (2.5b)$$

All the splitting functions in Eqs. (2.5a) and (2.5b) are listed in Appendix B. If the summation over i is taken in Eq. (2.5a), it becomes the evolution equation for the singlet distribution q_s :

$$\begin{aligned} \frac{\partial}{\partial t} \tilde{q}_s(x, t) = \int_x^1 \frac{dy}{y} \left[\left\{ \tilde{P}_{q^+, NS} \left(\frac{x}{y} \right) + 2N_f C_F T_R \tilde{F}_{qq} \left(\frac{x}{y} \right) \right\} \tilde{q}_s(y, t) \right. \\ \left. + N_f \tilde{P}_{qg} \left(\frac{x}{y} \right) \tilde{g}(y, t) \right] . \quad (2.6) \end{aligned}$$

The reason for writing the evolution equations in term of the flavor-dependent distribution q_i^+ instead of the singlet one q_s is because antiquark distributions are neither $SU(3)_{\text{flavor}}$ nor $SU(2)_{\text{flavor}}$ symmetric.

Next, we discuss NLO effects in the evolution equations. NLO effects are included in the coupling constant $\alpha_s(t)$, in the splitting functions $P_{p_i p_j}(z)$, and in coefficient functions. Explicit NLO expressions are given in appendices. It should be noted that the LO or NLO expression of $\alpha_s(Q^2)$ is used in the LO or NLO evolution case respectively in Eq. (2.1). Once the NLO corrections are included in the evolution, the renormalization scheme has to be specified. Throughout this paper, we use the \overline{MS} scheme. The splitting function is given by the LO and NLO ones as

$$P_{ij}(x) = P_{ij}^{(0)}(x) + \frac{\alpha_s(Q^2)}{2\pi} P_{ij}^{(1)}(x) . \quad (2.7)$$

Then the splitting functions $\tilde{P}_{ij}(z)$ in Eqs. (2.4a) and (2.4b) are

$$\tilde{P}_{ij}(x) = \tilde{P}_{ij}^{(0)}(x) + \frac{\alpha_s(t)}{2\pi} R_{ij}(x) , \quad (2.8)$$

where the function $R_{ij}(z)$ is

$$R_{ij}(x) \equiv \tilde{P}_{ij}^{(1)}(x) - \frac{\beta_1}{2\beta_0} \tilde{P}_{ij}^{(0)}(x) . \quad (2.9)$$

The second term in Eq. (2.9) appears because of the transformation from Q^2 to t . To be precise, the splitting functions \tilde{P}_{ij} in Eqs. (2.3)–(2.6) and (2.8) should be denoted, for example, \tilde{P}'_{ij} because it is different from $xP_{ij} = xP_{ij}^{(0)} + (\alpha_s/2\pi)xP_{ij}^{(1)}$. However, we omit the prime throughout this paper for using simpler notations.

We discussed the evolution equations for quark and gluon distributions. In calculating structure functions, a correction due to the NLO coefficient function should be taken into account. In the nonsinglet case, it is given by

$$\tilde{F}_n^{NS}(x, Q^2) = \int_x^1 \frac{dy}{y} \tilde{C}_n^q\left(\frac{x}{y}, \alpha_s\right) \tilde{q}_n^{NS}(y, Q^2) \quad , \quad (2.10)$$

where n denotes the type of a structure function, $\tilde{F}_n = xF_1$, F_2 , or xF_3 for $n=1, 2$, or 3 respectively, and C_n^q is a quark coefficient function. In the singlet case or in the q_i^+ case, an additional gluon correction term should be taken into account:

$$\tilde{F}_{n,i}^+(x, Q^2) = \int_x^1 \frac{dy}{y} \tilde{C}_n^q\left(\frac{x}{y}, \alpha_s\right) \tilde{q}_i^+(y, Q^2) + \int_x^1 \frac{dy}{y} \tilde{C}_n^g\left(\frac{x}{y}, \alpha_s\right) \tilde{g}(y, Q^2) \quad , \quad (2.11)$$

where C_n^g is a gluon coefficient function. C_n^q and C_n^g are given in Appendix C. The Q^2 evolution of a quark distribution is first calculated, then the structure function at Q^2 is evaluated by using the convolution integrals in Eq. (2.10) or (2.11), so that this method is called “two-step evolution”.

The above procedure requires an initial quark (and gluon) distribution for getting a structure function at certain Q^2 . It cannot be used for the NLO evolution if a structure function is given as the initial distribution. In such a case, “one-step-evolution” equations for the structure function are useful. They are derived from the evolution equations and the convolution equations with the coefficient functions. The nonsinglet equation is in the same form with Eqs. (2.3) and (2.8) [6]:

$$\frac{\partial}{\partial t} \tilde{F}_{NS}(x, t) = \int_x^1 \frac{dy}{y} \left[\tilde{P}_{NS}^{(0)}\left(\frac{x}{y}\right) + \frac{\alpha_s(t)}{2\pi} R_{NS}\left(\frac{x}{y}\right) \right] \tilde{F}_{NS}(y, t) \quad , \quad (2.12)$$

except for taking

$$R_{NS}(x) = \tilde{P}_{NS}^{(1)}(x) - \frac{\beta_1}{2\beta_0} \tilde{P}_{NS}^{(0)}(x) - \frac{\beta_0}{4} \tilde{B}_n^q(x) \quad . \quad (2.13)$$

$B_n^q(x)$ ($n=1, 2$, or 3) is the α_s correction in the coefficient function in Appendix C. Using the above one-step equation, we can evolve the nonsinglet structure function itself. In the similar way, the one-step F_i^+ evolution equation is given by [8]

$$\frac{\partial}{\partial t} \begin{pmatrix} \tilde{F}_i^+(x, t) \\ \tilde{g}(x, t) \end{pmatrix} = \int_x^1 \frac{dy}{y} \left[\tilde{\mathbf{P}}^{(0)}\left(\frac{x}{y}\right) + \frac{\alpha_s(t)}{2\pi} \mathbf{R}\left(\frac{x}{y}\right) \right] \begin{pmatrix} \tilde{F}_j^+(y, t) \\ \tilde{g}(y, t) \end{pmatrix} \quad , \quad (2.14)$$

with

$$\mathbf{R}(x) = \tilde{\mathbf{P}}^{(1)}(x) - \frac{\beta_1}{2\beta_0} \tilde{\mathbf{P}}^{(0)}(x) - \frac{\beta_0}{4} \tilde{\mathbf{D}}^{(1)}(x) + \tilde{\mathbf{E}}(x) \quad . \quad (2.15)$$

$\mathbf{P} = \tilde{\mathbf{P}}/x$, $\mathbf{D}^{(1)} = \tilde{\mathbf{D}}^{(1)}/x$, and $\mathbf{E} = \tilde{\mathbf{E}}/x$ are given by

$$\mathbf{P}^{(0),(1)}(x) = \begin{pmatrix} \sum_j P_{q_i^+ q_j^+}^{(0),(1)}(x) & P_{qg}^{(0),(1)}(x) \\ \sum_j P_{gq_j^+}^{(0),(1)}(x) & P_{gg}^{(0),(1)}(x) \end{pmatrix}, \quad (2.16)$$

$$\mathbf{D}^{(1)}(x) = \begin{pmatrix} B_n^q(x) & B_n^g(x) \\ 0 & 0 \end{pmatrix}, \quad (2.17)$$

and

$$\mathbf{E}(x) = \begin{pmatrix} E_{qq}(x) & E_{qg}(x) \\ E_{gq}(x) & E_{gg}(x) \end{pmatrix}. \quad (2.18)$$

Each matrix element in Eqs. (2.16), (2.17), and (2.18) is given in Appendix B. It should be mentioned that the above one-step-evolution equation is slightly different from the one in Ref. [8]. This discrepancy is because we use a convention for the momentum conservation, $\int_0^1 dx [\sum_i x(q_i + \bar{q}_i) + xg] = 1$, which is different from the one used by Herrod, Wada, and Webber, $\int_0^1 dx [F_S + xg'] = 1$. Therefore, the matrices $\mathbf{D}^{(1)}$ and \mathbf{E} are different from those listed in their paper.

2.2 Modified evolution equations due to recombinations (Mueller-Qiu equations)

The Altarelli-Parisi evolution equations have been used extensively and they have been successful in describing many experimental data. However, as it becomes possible to reach the small x region by high-energy accelerators, it is necessary to investigate the details of small x physics. The gluon distribution $g(x, Q^2)$ is a measurement of a gluon with transverse size $\sim 1/\sqrt{Q^2}$, and the number of gluons per unit rapidity is $xg(x, Q^2)$. If $xg(x, Q^2)/Q^2 \ll R_0^2$ (R_0 =nucleon size) is satisfied, gluon interactions are neglected and the Altarelli-Parisi equations in Eqs. (2.3), (2.4), (2.5), and (2.6) can be used for the Q^2 evolution. However, if the transverse area $xg(x, Q^2)/Q^2$ exceed the nucleon size $\sim R_0^2$, gluons within a unit of rapidity spatially overlap, and the gluons are no longer considered as free partons. If the gluon density becomes large $xg(x, Q^2) \gtrsim R_0^2 Q^2$, the gluon interactions should be taken into account. These interactions are called parton recombinations, which are also used for explaining nuclear shadowing [4]. There are a number of studies on the recombinations. Among them, we employ the evolution equations proposed by Mueller and Qiu [2]. They investigated gluon-gluon recombination effects on the evolution, and they proposed the following modified evolution equations:

$$\begin{aligned}
\frac{\partial}{\partial t} \tilde{q}_i^+(x, t) = & \int_x^1 \frac{dy}{y} \left[\tilde{P}_{q^+, NS} \left(\frac{x}{y} \right) \tilde{q}_i^+(y, t) + 2C_F T_R \tilde{F}_{qq} \left(\frac{x}{y} \right) \tilde{q}_s(y, t) \right. \\
& \left. + \tilde{P}_{qg} \left(\frac{x}{y} \right) \tilde{g}(y, t) \right] \\
& - 2 \frac{K}{\pi R_0^2} \frac{1}{Q^2} \left\{ \frac{(2\pi)^2 \alpha_s(t)}{N_c(N_c^2 - 1)} \left(\frac{4}{15} N_c^2 - \frac{3}{5} \right) [\tilde{g}(x, t)]^2 \right. \\
& \left. + \int_x^1 \frac{dy}{y} \tilde{P}_{qg} \left(\frac{x}{y} \right) \tilde{G}_{HT}(y, t) \right\} \quad , \quad (2.19a)
\end{aligned}$$

$$\begin{aligned}
\frac{\partial}{\partial t} \tilde{q}_s(x, t) = & \int_x^1 \frac{dy}{y} \left[\left\{ \tilde{P}_{q^+ NS} \left(\frac{x}{y} \right) + 2N_f C_F T_R \tilde{F}_{qq} \left(\frac{x}{y} \right) \right\} \tilde{q}_s(y, t) \right. \\
& \left. + N_f \tilde{P}_{qg} \left(\frac{x}{y} \right) \tilde{g}(y, t) \right] \\
& - 2N_f \frac{K}{\pi R_0^2} \frac{1}{Q^2} \left\{ \frac{(2\pi)^2 \alpha_s(t)}{N_c(N_c^2 - 1)} \left(\frac{4}{15} N_c^2 - \frac{3}{5} \right) [\tilde{g}(x, t)]^2 \right. \\
& \left. + \int_x^1 \frac{dy}{y} \tilde{P}_{qg} \left(\frac{x}{y} \right) \tilde{G}_{HT}(y, t) \right\} \quad , \quad (2.19b)
\end{aligned}$$

$$\begin{aligned}
\frac{\partial}{\partial t} \tilde{g}(x, t) = & \int_x^1 \frac{dy}{y} \left[\tilde{P}_{gq^+} \left(\frac{x}{y} \right) \tilde{q}_s(y, t) + \tilde{P}_{gg} \left(\frac{x}{y} \right) \tilde{g}(y, t) \right] \\
& - \frac{K}{\pi R_0^2} \frac{1}{Q^2} \left\{ \frac{8\pi^2}{N_c^2 - 1} \alpha_s(t) C_G^2 \int_x^1 \frac{dy}{y} [\tilde{g}(y, t)]^2 \right\} \quad , \quad (2.19c)
\end{aligned}$$

where $\tilde{G}_{HT}(x, t)$ is a higher-dimensional distribution, which follows the evolution equation:

$$\frac{\partial}{\partial t} \tilde{G}_{HT}(x, t) = \frac{8\pi^2}{N_c^2 - 1} \alpha_s(t) C_G^2 \int_x^1 \frac{dy}{y} [\tilde{g}(y, t)]^2 \quad . \quad (2.19d)$$

In order to solve this equation, the initial \tilde{G}_{HT} distribution has to be supplied. Because \tilde{G}_{HT} is associated with the two gluon interactions, we may assume

$$\tilde{G}_{HT}(x, Q_0^2) = K_{HT} [\tilde{g}(x, Q_0^2)]^2 \quad , \quad (2.20)$$

where K_{HT} is a constant. In Eq. (2.19a, b, c), R_0 is the nucleon size, N_f is the number of flavor, N_c is the number of color, and $K=9/8$ so that nuclear correction terms vanish for $A=1$ [See Eqs. (2.22a, b, c)]. The splitting function $\tilde{P}_{qg}(z)$ is given in Appendix B. The recombination contributions enter into the evolution in the same α_s order as the next-to-leading order in the splitting function, so that the NLO effects in the Altarelli-Parisi evolution terms should be included.

We comment on additional terms in Eq. (2.19). For the details the recombination processes, we refer the reader to the original paper [2]. The recombination terms are related to the two-gluon density, $G^{(2)}(x, Q^2) = G^{(2)}(x_1, x_2, p_{1T}^2, p_{2T}^2)$ with $x_1 = x_2 = x$ and $p_{1T}^2 = p_{2T}^2 = Q^2$. Because the normalization of the two-gluon density is given by $G^{(2)}(x_1, x_2, p_{1T}^2, p_{2T}^2) = (3R_0\bar{n}_0/2)g(x_1, p_{1T}^2)g(x_2, p_{2T}^2)$ with $\bar{n}_0 = 3/4\pi R_0^3$, it becomes $G^{(2)}(x, Q^2) = (3R_0\bar{n}_0/2)[g(x, Q^2)]^2$, which are the $[g(x, Q^2)]^2$ terms in Eq. (2.19). It results in the recombination factor, which is proportional to $R_0\bar{n}_0\alpha_s/Q^2 = 3\alpha_s/(4\pi R_0^2 Q^2)$. The factor α_s/Q^2 arises because a parton-parton fusion cross section is proportional to α_s/Q^2 . This extra $1/Q^2$ dependence is an interesting higher-twist effect, which could be investigated experimentally at small x and at small Q^2 . The $1/R_0^2$ factor arises due to the integration over the intrinsic transverse momentum.

In the case of nuclear parton distributions, there are additional terms due to parton recombinations from different nucleons. Parton distributions in a nucleus are defined by

$$\tilde{p}^A(x, t) = \tilde{p}(x, t) - \delta\tilde{p}^A(x, t) \quad , \quad (2.21)$$

where nuclear distributions are expressed by those per nucleon. The evolution of the first term is given in Eq. (19). The evolution of the nuclear correction terms is obtained by solving

$$\begin{aligned} \frac{\partial}{\partial t} \delta\tilde{q}_i^{+,A}(x, t) = & \int_x^1 \frac{dy}{y} \left[\tilde{P}_{q^+, NS} \left(\frac{x}{y} \right) \delta\tilde{q}_i^{+,A}(y, t) + 2C_F T_R \tilde{F}_{qq} \left(\frac{x}{y} \right) \delta\tilde{q}_s^A(y, t) \right. \\ & \left. + \tilde{P}_{qg} \left(\frac{x}{y} \right) \delta\tilde{g}^A(y, t) \right] \quad , \\ & + 2 \left(\frac{3}{2} R_A \bar{n} - \frac{K}{\pi R_0^2} \right) \frac{1}{Q^2} \left\{ \frac{(2\pi)^2 \alpha_s(t)}{N_c(N_c^2 - 1)} \left(\frac{4}{15} N_c^2 - \frac{3}{5} \right) [\tilde{g}(x, t)]^2 \right. \\ & \left. + \int_x^1 \frac{dy}{y} \tilde{P}_{qg} \left(\frac{x}{y} \right) \tilde{G}_{HT}(y, t) \right\} \quad , \quad (2.22a) \end{aligned}$$

$$\begin{aligned} \frac{\partial}{\partial t} \delta\tilde{q}_s^A(x, t) = & \int_x^1 \frac{dy}{y} \left[\left\{ \tilde{P}_{q^+, NS} \left(\frac{x}{y} \right) + 2N_f C_F T_R \tilde{F}_{qq} \left(\frac{x}{y} \right) \right\} \delta\tilde{q}_s^A(y, t) \right. \\ & \left. + N_f \tilde{P}_{qg} \left(\frac{x}{y} \right) \delta\tilde{g}^A(y, t) \right] \\ & + 2N_f \left(\frac{3}{2} R_A \bar{n} - \frac{K}{\pi R_0^2} \right) \frac{1}{Q^2} \left\{ \frac{(2\pi)^2 \alpha_s(t)}{N_c(N_c^2 - 1)} \left(\frac{4}{15} N_c^2 - \frac{3}{5} \right) [\tilde{g}(x, t)]^2 \right. \\ & \left. + \int_x^1 \frac{dy}{y} \tilde{P}_{qg} \left(\frac{x}{y} \right) \tilde{G}_{HT}(y, t) \right\} \quad , \quad (2.22b) \end{aligned}$$

$$\begin{aligned}
\frac{\partial}{\partial t} \delta \tilde{g}^A(x, t) = & \int_x^1 \frac{dy}{y} \left[\tilde{P}_{gq^+} \left(\frac{x}{y} \right) \delta \tilde{q}_s^A(y, t) + \tilde{P}_{gg} \left(\frac{x}{y} \right) \delta \tilde{g}^A(y, t) \right] \\
& + \left(\frac{3}{2} R_A \bar{n} - \frac{K}{\pi R_0^2} \right) \frac{1}{Q^2} \left\{ \frac{8\pi^2}{N_c^2 - 1} \alpha_s(t) C_G^2 \int_x^1 \frac{dy}{y} [\tilde{g}(y, t)]^2 \right\} .
\end{aligned} \tag{2.22c}$$

where \bar{n} is the number density $\bar{n} = 3A/(4\pi R_A^3)$. Nuclear radius is given by $R_A = R_1 A^{1/3}$ with $R_1 = 1.1$ fm. For simplicity, we take $R_0 = R_1 = 1$ fm and $K = 9/8$ so that the nuclear correction terms in Eqs. (2.22a, b, c) vanish at $A = 1$. We note that two parton number density is $T_{12}(x_1, x_2, Q^2) = (3/2) R_A \bar{n} p_1(x_1) p_2(x_2)$. Therefore, the overall A dependence is $R_A \bar{n} \propto A^{1/3}$, which is just the number of nucleons in the longitudinal direction.

3. Brute-force method

It is useful to have a computer program of solving the evolution equations accurately because they are frequently used in theoretical and experimental studies. There are a number of methods such as Mellin-transformation and orthogonal-polynomial methods [5]. We have been studying a Laguerre-polynomial method and it is very efficient by considering computing time and numerical accuracy [6]. However, the results are slightly worse in the nonsinglet case, particularly at small and large x . Furthermore, the evolution equations with the recombinations have complex nonlinear terms, which cannot be handled properly by the Laguerre polynomials. In addition to these issues, parton distributions with singular behavior at small x ($x p(x) \rightarrow \infty$ as $x \rightarrow 0$) could not be evolved either in the program LAG1 nor in LAG2NS [6]. The singular behavior in sea-quark and gluon distributions attracts much attention recently due to the HERA F_2 experimental data.

Taking these difficulties into consideration, we decide to employ a brute-force method [7]. The variables x and t are divided into small steps and integration and differentiation are defined by $df(x)/dx = [f(x_{m+1}) - f(x_m)]/\Delta x_m$ and $\int dx f(x) = \sum_{m=1}^{N_x} \Delta x_m f(x_m)$. Then, the evolution equations could be solved rather easily. For example, Eq. (2.3) is written in the following form:

$$\tilde{q}_{NS}(x_k, t_{j+1}) = \tilde{q}_{NS}(x_k, t_j) + \Delta t_j \sum_{m=k}^{N_x} \frac{\Delta x_m}{x_m} \tilde{P}_{NS}\left(\frac{x_k}{x_m}\right) \tilde{q}_{NS}(x_m, t_j) \quad . \quad (3.1)$$

If the initial distribution $\tilde{q}_{NS}(x_m, t_{j=1})$ is given, the distribution at $t_1 = \Delta t$ is calculated in the above equation. Repeating this step $N_t - 1$ times, we obtain the final distribution at t_{N_t} . This method is very simple but N_x and N_t have to be large enough to get accurate results. However, we can reasonably expect that N_t does not have to be very large. This is because the scaling of structure functions works approximately, and they depend on the variable t weakly. On the other hand, N_x has to be fairly large. Numerical problems are expected at small x if the x step is taken in the linear scale ($\Delta x = 1/N_x$). The small x region becomes increasingly important with the development of high-energy accelerators such as HERA. So it is necessary to have a good numerical method at small x as small as 10^{-4} . In order to satisfy this condition, the logarithmic- x step $\Delta(\log_{10} x) = |\log_{10} x_{min}|/N_x$ is taken in our analysis.

The singlet and q_i^+ evolution equations in Eqs. (2.5a), (2.5b), and (2.6) are more complex, but they can be solved in the similar way. These equations are written in the brute-force method as:

$$\begin{aligned}
\tilde{q}_i^+(x_k, t_{j+1}) &= \tilde{q}_i^+(x_k, t_j) + \Delta t_j \sum_{m=k}^{N_x} \frac{\Delta x_m}{x_m} \tilde{P}_{q^+, NS} \left(\frac{x_k}{x_m} \right) \tilde{q}_i^+(x_m, t_j) \\
&+ \Delta t_j \sum_{m=k}^{N_x} \frac{\Delta x_m}{x_m} 2C_F T_R \tilde{F}_{qq} \left(\frac{x_k}{x_m} \right) \tilde{q}_s(x_m, t_j) + \Delta t_j \sum_{m=k}^{N_x} \frac{\Delta x_m}{x_m} \tilde{P}_{qg} \left(\frac{x_k}{x_m} \right) \tilde{g}(x_m, t_j) \quad , \\
\end{aligned} \tag{3.2a}$$

$$\begin{aligned}
\tilde{q}_s(x_k, t_{j+1}) &= \tilde{q}_s(x_k, t_j) + \Delta t_j \sum_{m=k}^{N_x} \frac{\Delta x_m}{x_m} \left[\tilde{P}_{q^+, NS} \left(\frac{x_k}{x_m} \right) + 2N_f C_F T_R \tilde{F}_{qq} \left(\frac{x_k}{x_m} \right) \right] \tilde{q}_s(x_m, t_j) \\
&+ \Delta t_j \sum_{m=k}^{N_x} \frac{\Delta x_m}{x_m} \tilde{P}_{qg} \left(\frac{x_k}{x_m} \right) \tilde{g}(x_m, t_j) \quad , \quad (3.2b)
\end{aligned}$$

$$\begin{aligned}
\tilde{g}(x_k, t_{j+1}) &= \tilde{g}(x_k, t_j) + \Delta t_j \sum_{m=k}^{N_x} \frac{\Delta x_m}{x_m} \tilde{P}_{gq} \left(\frac{x_k}{x_m} \right) \tilde{q}_s(x_m, t_j) \\
&+ \Delta t_j \sum_{m=k}^{N_x} \frac{\Delta x_m}{x_m} \tilde{P}_{gg} \left(\frac{x_k}{x_m} \right) \tilde{g}(x_m, t_j) \quad . \quad (3.2c)
\end{aligned}$$

If the initial distributions, $\tilde{q}_i^+(x_m, t_{j=0})$, $\tilde{q}_s(x_m, t_{j=0})$, and $\tilde{g}(x_m, t_{j=0})$ are provided, evolved distributions at $t_1 = \Delta t$ are calculated in the above equations. Repeating this step $N_t - 1$ times, we obtain the final evolved distributions. The other evolution equations in section 2 can be solved in the same way.

We did not write explicitly the integrals associated with $1/(1-x)_+$ terms in Eq. (3.2). However, special care has to be taken in calculating the $1/(1-x)_+$ terms in the splitting functions. The $+$ function is defined in the integral region ($0 \leq x \leq 1$) [Eq. (B.2)], so that the integral is given in the brute-force method as

$$\int_x^1 dx' \frac{f(x')}{(1-x')_+} = \sum_{m=k}^{N_x} \Delta x_m \frac{f(x_m) - f(1)}{1 - x_m} + f(1) \ln(1 - x_k) \quad . \quad (3.3)$$

The integral with $[\ln(1-x)/(1-x)]_+$ is given in the similar way:

$$\int_x^1 dx' f(x') \left[\frac{\ln(1-x')}{1-x'} \right]_+ = \sum_{m=k}^{N_x} \Delta x_m [f(x_m) - f(1)] \frac{\ln(1-x_m)}{1-x_m} + \frac{1}{2} f(1) \ln^2(1-x_k) \quad . \quad (3.4)$$

While the nonlinear recombination terms are difficult to be handled in the Laguerre method, it is straightforward to include them in the brute-force method. In addition, there is no evolution problem due to the singular behavior of parton distributions at small x , because all calculations in Eqs. (3.1) and (3.2) could be done in the x region, $x \geq x_{min}$. x_{min} is set for 10^{-4} in our analysis, but it could be varied depending on one's interest. Because the recombination equations in section 2.2 are solved in the similar way, we do not write corresponding expressions in the brute-force method.

4. Description of input parameters and input distributions

For running the FORTRAN-77 program BF1, a user should supply twenty-one input parameters from the file #10. In addition, an input distribution(s) should be given in a function subroutine(s) in the end of the FORTRAN program or in an input data file(s), #13, #14, #15, #16, and/or #17. Evolution results are written in the output file #11. We explain the input parameters and the input distributions in the following.

4.1 Input parameters

There are twenty-one input parameters. Numerical values of the parameters should be supplied in the file #10, then these are read in the main program.

- (1) IOUT = 1, write x and $xq_{NS}(x)$ [or $xF_{NS}(x)$] at fixed Q^2 (=Q2) in the file #11;
 = 2, write Q^2 and $xq_{NS}(Q^2)$ [or $xF_{NS}(Q^2)$] at fixed x (=XX) in the file #11;
 = 3, x , $xq_s(x)$ [or $xF_s(x)$], and $xg(x)$;
 = 4, Q^2 , $xq_s(Q^2)$ [or $xF_s(Q^2)$], and $xg(Q^2)$;
 = 5, x , $xq_i^+(x)$ [or $xF_i^+(x)$], $xq_s(x)$ [or $xF_s(x)$], and $xg(x)$;
 = 6, Q^2 , $xq_i^+(Q^2)$ [or $xF_i^+(Q^2)$], $xq_s(Q^2)$ [or $xF_s(Q^2)$], and $xg(Q^2)$.
- (2) INPUT = 1, parton distributions in the nucleon;
 = 2, parton distributions in a nucleus.
 Note: If MODIFY=2 and INPUT=2 are chosen, parton distributions both in a nucleus and in the nucleon should be supplied.
- (3) IREAD = 1, give initial distribution(s) in function subroutine(s);
 = 2, read initial distribution(s) from data file(s).
- (4) MODIFY = 1, Altarelli-Parisi Q^2 evolution;
 = 2, Q^2 evolution with parton recombinations (Mueller-Qiu).
- (5) INDIST = 1, do not write initial distribution(s);
 = 2, write initial distribution(s) in the file #12;
 = 3, write initial distribution(s) in the file #12 without calculating evolution.
- (6) IORDER = 1, leading order in α_s ;
 = 2, next-to-leading order.
- (7) ITYPE = 1, structure function $xF_1(x, Q^2)$;
 = 2, $F_2(x, Q^2)$;
 = 3, $xF_3(x, Q^2)$;
 = 4, quark distribution $xq(x, Q^2)$.
 ITYPE determines the output distribution type.

- (8) ISTEP = 1, one-step evolution: $xq(Q_0^2) \rightarrow xq(Q^2)$ [or $xF(Q_0^2) \rightarrow xF(Q^2)$],
 $xg(Q_0^2) \rightarrow xg(Q^2)$;
note: one-step $xF_{1,S}$ evolution is not supplied;
= 2, two-step evolution: $xq(Q_0^2) \rightarrow xq(Q^2) \rightarrow xF(Q^2)$,
 $xg(Q_0^2) \rightarrow xg(Q^2)$.
- (9) IMORP = 1, $q_i - \bar{q}_i$ type distribution;
= 2, $q_i + \bar{q}_i$ type distribution.
- (10) Q02 = initial Q^2 ($\equiv Q_0^2$ in GeV^2) at which an initial distribution is supplied.
- (11) Q2 = Q^2 to which the distribution is evolved ($Q^2 \neq Q_0^2$).
- (12) DLAM = QCD scale parameter Λ_{QCD} in GeV .
- (13) NF = number of quark flavors (NF=3 or 4).
- (14) XX = x at which Q^2 dependent distributions are written (IOUT=2, 4, or 6 case).
- (15) NX = number of x steps (NX<5000).
- (16) NT = number of t steps (NT<5000).
- (17) NSTEP = number of x steps or t steps for writing output distribution(s).
- (18) NXMIN = $\log_{10}(\text{minimum of } x)$ [$0 < \min(x) = 10^{NXMIN} < XX$].
- (19) NA = mass number of a nucleus (NA=1 in the nucleon case).
- (20) RFM = $R_0=R_1$ (fm) in Eqs. (2.19) and (2.22).
- (21) DKHT = K_{HT} in $G_{HT}(x)$ in Eq. (2.20).
($G_{HT}(x)$ is a higher dimensional gluon distribution).

The meaning of IREAD is explained in section 4.2. IMORP=1 or 2 means that the distribution is $\sum_i a_i(q_i + \bar{q}_i)$ or $\sum_i a_i(q_i - \bar{q}_i)$ type, where a_i are constants. For example, $u_v + d_v = (u - \bar{u}) + (d - \bar{d})$ and $F_3^{\nu p} + F_3^{\bar{\nu} p}$ are $q_i - \bar{q}_i$ type distributions. F_2^{ep} is obtained by the convolution of the distributions, $(4/9)x(u + \bar{u} + c + \bar{c}) + (1/9)x(d + \bar{d} + s + \bar{s})$ and xg , with the corresponding coefficient functions, so that it is a $q_i + \bar{q}_i$ type distribution. In the evolution of nucleon structure functions, NA=1 should be supplied. In the Altarelli-Parisi evolution, the constants RKM and $DKHT$ are unnecessary so that arbitrary constants may be supplied.

For example, if one would like to evolve an initial singlet-quark distribution xq_s at $Q^2=4 \text{ GeV}^2$ in the nucleon to the singlet structure function $F_{2,S}$ at $Q^2=200 \text{ GeV}^2$ by the NLO Altarelli-Parisi with $N_f=4$ and $\Lambda=0.255 \text{ GeV}$, the input parameters could be IOUT=3, INPUT=1, IREAD=1, MODIFY=1, INDIST=1, IORDER=2, ITYPE=2, ISTEP=2, IMORP=2, Q02=4.0, Q2=200.0, DLAM=0.255, NF=4, XX=0.0, NX=1000, NT=200, NSTEP=100, NXMIN=-4, NA=1, RFM=0.0, and DKHT=0.0. In this case, the input file #10 is the following.

3, 1, 1, 1, 1, 2, 2, 2, 2
4.0, 200.0, 0.255, 4, 0.0, 1000, 200, 100, -4, 1, 0.0, 0.0

4.2 Input distributions supplied by function subroutines (IREAD=1)

If IREAD=1 is chosen, an input distribution(s) at Q_0^2 should be supplied in the end of the FORTRAN program BF1 as a function subroutine(s).

1) Nonsinglet case in the nucleon and nuclei

An initial nonsinglet-quark distribution (or a nonsinglet structure function) at Q_0^2 should be given in QNS0(X) as a double precision function. As an example, the MRS(G) valence quark distribution $xu_v + xd_v$ [10] at $Q_0^2=4 \text{ GeV}^2$ is given in the original program BF1.

2) Singlet case in the nucleon

An initial singlet-quark distribution (or a singlet structure function) in the nucleon at Q_0^2 should be supplied in QS0(X), and an initial gluon distribution in the nucleon should be in G0(X). These subroutines are used in the nucleon case and also in the nuclear case with MODIFY=2. The MRS(G) $xq_s = xu_v + xd_v + xS$ and xg distributions are given.

3) q_i^+ (F_i^+) distribution case in the nucleon

An initial q_i^+ distribution (or F_i^+) in the nucleon at Q_0^2 should be supplied in QI0(X), a singlet-quark distribution (or a singlet structure function) in the nucleon should be in QS0(X), and an initial gluon distribution in the nucleon should be in G0(X). These subroutines are used in the nucleon case and also in the nuclear case with MODIFY=2. The MRS(G) distributions are given in each function subroutine. $xq_i^+ = xd + x\bar{d}$ is given as an example.

4) Singlet case in a nucleus

An initial nuclear singlet-quark distribution (or a singlet structure function) at Q_0^2 should be supplied in QSA0(X), and a nuclear gluon distribution should be in GA0(X). These subroutines are used only in the nuclear case. The SK xq_s^{Ca} and xg^{Ca} distributions [4] are given as an example.

5) q_i^+ (F_i^+) distribution case in a nucleus

An initial nuclear q_i^+ distribution (or F_i^+) at Q_0^2 should be supplied in QIA0(X), a nuclear singlet-quark distribution (or a singlet structure function) should be in QSA0(X), and an nuclear gluon distribution should be in GA0(X). These subroutines are used only in the nuclear case. The SK distributions are given in each function subroutine.

4.3 Input distributions supplied by data files (IREAD=2)

If IREAD=2 is chosen, an input distribution(s) at Q_0^2 should be supplied in a separate data file(s).

1) Nonsinglet case in the nucleon and nuclei (data file #13)

An initial nonsinglet-quark distribution (or a nonsinglet structure function) at Q_0^2 should be given in the data file #13 as shown in the following example.

0.000100	0.023868
0.000110	0.024942
0.000120	0.026069
0.000132	0.027251
0.000145	0.028491
...	...
...	...
...	...
1.000000	0.000000

The first column is the x values and the second one is the corresponding $xu_v + xd_v$ values. The data at $x \leq x_{min}$ and at $x=1.0$ must be supplied.

2) Singlet case in the nucleon (data file #14)

An initial singlet-quark distribution (or a singlet structure function) and a gluon distribution should be given in the data file #14 as shown in the following.

0.000100	3.137921	23.163731
0.000110	3.114648	22.485543
0.000120	3.091368	21.825121
0.000132	3.068077	21.181969
0.000145	3.044768	20.555604
...
...
...
1.000000	0.000000	0.000000

The first column is the x values, the second is the xq_s distribution, and the third is the xg distribution. The data at $x \leq x_{min}$ and at $x=1.0$ must be supplied.

3) q_i^+ (F_i^+) distribution case in the nucleon (data file #15)

An initial q_i^+ distribution (or F_i^+), a singlet-quark distribution (or a singlet structure function), and a gluon distribution should be given in the data file #15 as shown in the following.

0.000100	1.229377	3.137921	23.163731
0.000110	1.220390	3.114648	22.485543
0.000120	1.211413	3.091368	21.825121
0.000132	1.202445	3.068077	21.181969
0.000145	1.193483	3.044768	20.555604
...
...
...
1.000000	0.000000	0.000000	0.000000

The first column is the x values, the second is the xu^+ distribution, the third is xq_s , and the fourth is xg . The data at $x \leq x_{min}$ and at $x=1.0$ must be supplied.

4) Singlet case in a nucleus (data file #16)

An initial nuclear singlet-quark distribution (or a singlet structure function) and a nuclear gluon distribution should be given in the data file #16 as shown in the nucleon case 2). In the MODIFY=2 case, the nucleon data file #14 should be also supplied.

5) q_i^+ (F_i^+) distribution case in a nucleus (data file #17)

An initial nuclear q_i^+ distribution (or F_i^+), a nuclear singlet-quark distribution (or a singlet structure function), and a nuclear gluon distribution should be given in the data file #17 as shown in the nucleon case 3). In the MODIFY=2 case, the nucleon data file #15 should be also supplied.

5. Description of the program BF1

5.1 Main program BF1

The main program reads twenty-one input parameters from the input file #10. The parameters are checked by the subroutine ERR. If there is an error, the program stops. Then, t defined in Eq. (2.1) is evaluated. Spline coefficients of the Spence function in Eqs. (B.7) and (B.8) are calculated by calling the SPLINE subroutine, and the interpolated function is used throughout the program for saving computation time. In the end, GETQNS is called in the nonsinglet case and GETQS is called in the singlet (or xq^+ , xF^+) case for calculating the Q^2 evolution.

5.2 Subroutine GETQNS

First, the initial distribution is taken from the subroutine QNS0 or is read from the file #13, and it is stored in the array QNS(I). The distribution is written in the file #12 if INDIST \neq 1. The initial distribution is stored in the array WQNS(I). The evolved distribution at $t_1 = \Delta t$ is calculated by calling QNSXT and it is stored in QNS(I). The major part of the NS evolution calculation is done in the QNSXT subroutine. Next, QNS(I) at $t_1 = \Delta t$ is stored in WQNS(I). The distribution at $t_2 = 2\Delta t$ is calculated again by calling QNSXT and it is stored in QNS(I). Repeating this step, we obtain the final distribution at $t = N_t \Delta t$. The results are interpolated either in the variable t or in x and they are written in the output file #11.

5.3 Subroutine GETQS

The initial distributions, xq_s and xg (xq_i^+ , xq_s^A , xg^A , $xq_i^{+,A}$), are taken from the functions, QS0 and G0 (QI0, QSA0, GA0, QIA0) or from the file #14, #15, #16, or #17. The distributions are stored in the arrays, QS(I) and G(I) (QI(I), QSA(I), GA(I), QIA(I)), and they are written in the file #12 if INDIST \neq 1. The initial distributions are stored in WQS(I) and WG(I) (WQI(I), WDQS(I), WDG(I), WDQI(I), WGHT(I)) [see Eqs. (2.20) and (2.21) for xG_{HT} and $\delta(xp^A)$]. The evolved ones at $t_1 = \Delta t$ are calculated by calling GETQGX, and results are stored in QS(I) and G(I) (QI(I), QSA(I), GA(I), QIA(I)). Next, the evolution results are stored in WQS(I) and WG(I) (WQI(I), WDSQ(I), WDG(I), WDQI(I), WGHT(I)) and the evolution from $t_1 = \Delta t$ to $t_2 = 2\Delta t$ is calculated. Repeating this step, we obtain the final distributions at $t = N_t \Delta t$. The results are interpolated either in the variable t or in x and they are written in the output file #11.

5.4 Subroutines ERR(IERR), INVERT(NN,QQQ)

The subroutine ERR checks whether the input parameters are valid. If they are not valid, this subroutine returns IERR=1 in the main program. The subroutine INVERT reverses the array QQQ, namely QQQ(1) \rightarrow QQQ(NN), QQQ(2) \rightarrow QQQ(NN-1), ...,

QQQ(NN)→QQQ(1). This is used in the Q^2 devolution case ($Q^2 < Q_0^2$).

5.5 Functions *FUNQ2J(IORDER,ALPHA)* and *ALPHAN(QQ)*

The function FUNQ2J obtains the Q^2 from a given running coupling constants α_s within the range from $Q_0^2 - 0.01(\text{GeV}^2)$ to $Q^2 + 0.01(\text{GeV}^2)$ if $Q_0^2 < Q^2$ (from $Q^2 - 0.01$ to $Q_0^2 + 0.01$ if $Q^2 < Q_0^2$). This function is used in calculating Q^2 from given t . The function ALPHAN(QQ) obtains the NLO running coupling constant α_s at Q^2 in the \overline{MS} scheme.

5.6 Subroutine *GETQGX(ALPHA)*

The subroutine GETQGX calculates the singlet (and q_i^+ , F_i^+) evolution by calling functions, QSXT, GXT, QSKXT, GKXT, GHTXT, DQSXT, and DGXT, which corresponds to the evolution of xq_s (xq_i^+), xg , $xq_s(\text{recomb.})$, $xg(\text{recomb.})$, xG_{HT} , $\delta(xq_s)$ ($\delta(xq_i^+)$), and $\delta(xg)$. (or structure functions) respectively. In the Altarelli-Parisi evolution in the nucleon, only QSXT and GXT are called. In addition to these, QSKXT, GKXT, and GHTXT are called in the Mueller-Qiu case. DQSXT and DGXT are called in the nuclear case.

5.7 Subroutine *DELTA0(QGA,QG,DQG)*

This subroutine calculates the difference DQG between the nucleon parton distribution QG and the nuclear one QGA.

5.8 Functions *QSKXT(I,FF)* and *GKXT(I)*

These functions calculate recombination effects in the nucleon. QSKXT calculates the recombination terms in xq_s or xq_i^+ (or structure functions), and GKXT calculates the recombination in xg . The flavor number FF is used for obtaining either xq_s (FF= N_f) or xq_i^+ (FF=1).

5.9 Functions *QNSXT(I,ALPHA,IORDER,ITYPE,SIGN)*, *QSXT(I,ALPHA,QSK,WWQ,IORS,FF)*, *GXT(I,ALPHA,GK)*, *DQSXT(I,ALPHA,WWQ,IORS,FF)*, *DGXT(I,ALPHA)*

These function calculates the Q^2 evolution from t_j to $t_j + \Delta t$. QNSXT, QSXT, GXT, DQSXT, and DGXT calculate the evolution of nonsinglet-quark, singlet-quark, gluon, nuclear (actually, nuclear correction of) nonsinglet-quark, nuclear gluon distributions (and corresponding structure functions) respectively. The evolution in the brute-force method is discussed in detail in section 3. If IORS=1, the singlet distribution is calculated, and the xq_i^+ (xF_i^+) distribution is calculated if IORS=2.

5.10 Functions *PNS0(I,K,ZK)* and *PNS1(I,K,ZK,SIGN,WWQ)*

The function PNS0 (PNS1) calculates the LO (NLO) nonsinglet splitting function

multiplied by a nonsinglet quark distribution or a structure function, which is stored in WWQ. If IMORP=1 (SIGN=-1.0), PNS1 uses the “ $q - \bar{q}$ ” type splitting function, and it uses the “ $q + \bar{q}$ ” type splitting function if IMORP=2 (SIGN=+1.0).

5.11 Functions PSQ0(I,K,ZK,WWQ,WWG,FF), PSG0(I,K,ZK,WWQ,WWG), PSQ1(I,K,ZK,WWQI,WWQ,WWG,FF), and PSG1(I,K,ZK,WWQ,WWG)

These functions calculate splitting functions multiplied by quark and gluon distributions. The function PSQ0 calculates $\tilde{P}_{qq}^{(0)}(\frac{x}{y})WWQ + \tilde{P}_{gg}^{(0)}(\frac{x}{y})WWG$, where WWQ is $yq_s(y)$, $yF_s(y)$, $yq_i^+(y)$, or $yF_i^+(y)$ and WWG is $yg(y)$. The function PSG0 calculate $\tilde{P}_{qq}^{(0)}(\frac{x}{y})WWQ + \tilde{P}_{gg}^{(0)}(\frac{x}{y})WWG$. PSQ1 and PSG1 calculates the same quantities in NLO.

5.12 Functions CQ1(I,K,ZK,ITYPE,WWQ) and CG1(K,ZK,ITYPE,WWG)

The function CQ1 calculates the NLO coefficient function $C_q^{(1)}$ multiplied by a quark distribution or a structure function (WWQ). CG1 calculates $C_g^{(1)}$ multiplied by a gluon distribution (WWG). $C_q^{(1)}$ and $C_g^{(1)}$ are denoted B_n^q and B_n^g in Appendix C.

5.13 Functions EQQ(K,ZK,WWQ), EQG(K,ZK,WWG) and EGQ(K,ZK,WWQ)

These functions calculate E_{qq} , E_{qg} and E_{gq} multiplied by a structure function or a gluon distribution in the one-step evolution. $E_{gg} = -E_{qq}$ is used in calculating the E_{gg} part. See Appendix B for the explicit expressions of E_{qq} , E_{qg} and E_{gq} .

5.14 Function GHTXT(I)

This function calculates the evolution of the higher dimensional gluon distribution xG_{HT} from t_j to $t_j + \Delta t$ in Eq. (2.19d).

5.15 Subroutines GETFNS(ITYPE,ALPHA,QNS,FNS), GETF(IORS,ITYPE,ALPHA,QS,G,FS)

These subroutines calculate structure functions from quark and gluon distributions by taking convolutions with the coefficient functions. These are used in the two-step evolution. GETFNS obtains a nonsinglet structure function FNS from a nonsinglet quark distribution QNS. GETF obtains a singlet structure function (or xF_i^+) FS from singlet quark (or xq_i^+) and gluon distributions, QS and G.

5.16 Function *SPENCE(X)*

This function calculates the Spence function by using a series expansion form in Eq. (B.8). The upper limit of the summation is taken as $\max(k)=10000$ so that accuracy of the obtained function is better than 10^{-5} . The Spence function appears in the Splitting functions and it could take significant computing time if the function *SPENCE* is repeated called. Therefore, the interpolated one is used in calculating the splitting functions.

5.17 Subroutines *DATAR1(N,QFX)*, *DATAR2(N,QFX,GGX)*, *DATAR3(N,QIX,QFX,GGX)*

IF *IREAD*=2 is chosen, an initial distribution is read from a data file. *DATAR1* reads an initial nonsinglet distribution form the data file #N. *DATAR2* reads an initial singlet-quark distribution xq_s (or structure function xF_s) and a gluon distribution xg . *DATAR3* reads xq_i^+ (F_i^+), xq_s (xF_s), and xg . Then, the initial distribution data are interpolated, so that the reasonably large amount of data should be supplied in the file.

5.18 Subroutine *SPLINE(N,X,Y,B,C,D)* and function *SEVAL(N,XX,X,Y,B,C,D)*

The subroutine *SPLINE* calculates the coefficients, *B(I)*, *C(I)*, and *D(I)* ($I = 1, 2, \dots, N$) in a cubic Spline interpolation. *Y(I)* at *X(I)* ($I = 1, 2, \dots, N$) are supplied. This interpolation program is taken from Ref. [11]. Using the obtained Spline coefficients, the function *SEVAL* calculates the value of *Y* at given *XX*.

5.19 Functions *QQ(X,A,B,C)*, *QQMRS(X,A,B,C,D,E)*

These functions calculate typical parton distributions given by the parameters *A*, *B*, *C*, *D*, and *E*. *QQ* calculates $Ax^B(1-x)^C$, and *QQMRS* does $Ax^B(1+C\sqrt{x}+Dx)(1-x)^E$.

5.20 Functions *QNS0(X)*, *QS0(X)*, and *G0(X)*

The functions *QNS0*, *QS0*, and *G0* calculate an initial nonsinglet-quark distribution xq_{NS} (xF_{NS}), a singlet-quark distribution xq_s (xF_s), and a gluon distribution xg in the nucleon. As an example, the *MRS(G)* distributions [10] are provided. The nonsinglet one is $QNS0=xu_v + xd_v=2.704x^{0.593}(1-0.76\sqrt{x}+4.20x)(1-x)^{3.96}+0.2513x^{0.335}(1+8.63\sqrt{x}+0.32x)(1-x)^{4.41}$, the singlet one is $QS0=xu_v + xd_v + xS=2.704x^{0.593}(1-0.76\sqrt{x}+4.20x)(1-x)^{3.96}+0.2513x^{0.335}(1+8.63\sqrt{x}+0.32x)(1-x)^{4.41}+1.74x^{-0.067}(1-3.45\sqrt{x}+10.3x)(1-x)^{10.1}$, and the gluon distribution is $G0=1.51x^{-0.301}(1-4.14\sqrt{x}+10.1x)(1-x)^{6.06}$.

5.21 Functions $QSA0(X)$ and $GA0(X)$

The functions $QSA0$ and $GA0$ calculate a singlet-quark distribution xq_s (xF_s) and a gluon distribution xg in a nucleus. As an example, the SK distributions [4] at $Q_0^2=0.8 \text{ GeV}^2$ are provided. The singlet one is $QSA0=1.840x^{0.472}(1-0.984x)^{4.06}(1+9.33x)+6.423x^{0.600}(1-x)^{8.13}(1-0.568x)$, and the gluon distribution is $GA0=179.2x^{1.95}(1-x)^{7.32}(1-0.619x)$.

5.22 Functions $QI0(X)$ and $QIA0(X)$

The function $QI0$ or $QIA0$ calculates an initial distribution xq_i^+ (xF_i^+) in the nucleon or the one in a nucleus. As an example, the MRS(G) and SK xd^+ distributions are provided. The nucleon one is $QI0=+0.2513x^{0.335}(1+8.63\sqrt{x}+0.32x)(1-x)^{4.41}+0.4(1-0.02)1.74x^{-0.067}(1-3.45\sqrt{x}+10.3x)(1-x)^{10.1}+0.043x^{0.3}(1-x)^{10.1}(1+64.9x)$, and the nuclear one is $QIA0=1.773x^{0.656}(1-0.956x)^{5.23}(1+3.01x)+6.423x^{0.600}(1-x)^{8.13}(1-0.568x)/3$.

6. Numerical analysis

Parton distributions or structure functions either in the nucleon or in a nucleus could be evolved in the program BF1. We discuss numerical results on both cases.

6.1 Accuracy of Q^2 evolution results

We check the LO and NLO splitting functions, the coefficient functions, and the function \mathbf{E} by comparing their moments with other calculations in Refs. [8, 12, 13]. Because the different convention is employed for the gluon distribution from the one in Ref. [8], $\mathbf{D}^{(1)}$ and \mathbf{E} in Eqs. (2.17) and (2.18) are slightly different. We compare BF1 evolution results with the evolution of HMRS-B [14]. Choosing the HMRS-B singlet-quark and gluon distributions at $Q_0^2=4 \text{ GeV}^2$ as the initial distributions, we calculate the distributions at $Q^2=200 \text{ GeV}^2$ and compare them with the HMRS-B evolution results. We find that both agree well in the sense that the differences are typically within 2% in the region ($0.01 < x$). However, the differences become slightly larger at small x (2–4% at $0.0001 < x < 0.001$). We also checked various BF1 evolution results by comparing with those in the Laguerre polynomial method [6]. It indicates that both results agree within about 1% accuracy. Furthermore, we checked that results in the one-step evolution [$xF(x, Q_0^2) \rightarrow xF(x, Q^2)$] agree well with those in the two-step evolution [$xq(x, Q_0^2) \rightarrow xq(x, Q^2) \rightarrow xF(x, Q^2)$]. From these comparisons and repeated checks on the program, the program BF1 is believed to be a reliable evolution program. We discuss the details of numerical accuracy in the following.

First, Q^2 evolution of a nonsinglet distribution is calculated in the program BF1. There are essentially two parameters which determine numerical accuracy of the Q^2 evolution. These are numbers of points in variables x and t (N_x , N_t). We show dependency of our results on these numbers. For running the program BF1, the input parameters and an input distribution in section 4 should be supplied. As an initial nonsinglet distribution, we employ the HMRS-B $xu_v + xu_d$ at $Q_0^2=4 \text{ GeV}^2$. It is evolved up to $Q^2=200 \text{ GeV}^2$ with $\Lambda=0.19 \text{ GeV}$ and $N_f=4$.

In Fig. 1a, N_x is fixed at $N_x=1000$, then $N_t=10$, 20, or 500 is taken for finding the dependency on N_t . For example, the input parameters in the case of $N_t=500$ are IOUT=1, INPUT=1, IREAD=1, MODIFY=1, INDIST=2, IORDER=2, ITYPE=4, ISTEP=1, IMORP=1, Q02=4.0, Q2=200.0, DLAM=0.255, NF=4, XX=0.0, NX=1000, NT=500, NSTEP=100, NXMIN=-4, NA=1, RFM=0.0, and DKHT=0.0. There are solid, dashed, and dotted curves at $Q^2=200 \text{ GeV}^2$; however, these cannot be distinguished in Fig. 1. It indicates that numerical results are almost independent of the number N_t in the nonsinglet case if N_t is more than a certain number. This result is, in fact, anticipated because the scaling hypothesis works approximately in parton distributions. In comparison with the $N_t=500$ results, numerical differences are within 1% at $10^{-4} < x < 0.5$ and 4% at $x=0.8$ in the $N_t=10$ case, within 0.6% at $10^{-4} < x < 0.5$ and 2% at $x=0.8$ in $N_t=20$, and within 0.2% at $10^{-4} < x < 0.5$ and 0.8% at $x=0.8$ in

$N_t=50$.

Next, N_x is varied with the fixed $N_t=50$ in Fig. 1b. Four types of curves are shown at $Q^2=200$ GeV². The dotted curve is the evolution result for $N_x=100$, the dashed for $N_x=300$, the dot-dashed for $N_t=1000$, and the solid for $N_t=4000$. As it is shown in the figure, we should take rather larger number of N_x for getting converging results. The accuracy is worse if $N_x < 100$. In comparison with the $N_x=4000$ results, numerical differences are within 9% at $10^{-4} < x < 0.5$ and 24% at $x=0.8$ in the $N_x=100$ case, within 3% at $10^{-4} < x < 0.5$ and 8% at $x=0.8$ in $N_x=300$, and within 0.7% at $10^{-4} < x < 0.5$ and 2% at $x=0.8$ in $N_x=1000$.

From the above results, we recommend to use $N_t \geq 50$ and $N_x \geq 1000$ for getting accuracy better than 1% at $0.0001 < x < 0.5$ and better than 2% at $0.5 < x < 0.8$ in the nonsinglet case. Running CPU time with $N_t=50$ and $N_x=1000$ is about five minutes on the AlphaServer 2100 4/200.

Singlet distribution results are shown in Fig. 2a, where N_t is varied with fixed $N_x=1000$. The initial distributions are the HMRS-B singlet-quark and gluon distributions at $Q_0^2=4$ GeV². The dotted, dashed, dot-dashed, and solid curves are the results for $N_t=20, 50, 200$, and 1000 respectively. As it is obvious from the figure, we need to take large N_t for getting convergent results at small x . In comparison with the $N_t=1000$ results, numerical differences are within 5% at $10^{-4} < x < 0.9$ in the $N_t=20$ case, within 2% at $10^{-4} < x < 0.9$ in $N_t=50$, and within 0.4% at $10^{-4} < x < 0.9$ in $N_t=200$. In Fig. 2b, N_x is varied with fixed $N_t=200$ in the singlet distribution. The dotted, dashed, dot-dashed, and solid curves are obtained by taking $N_x=100, 300, 1000$, and 4000 respectively. In comparison with the $N_x=4000$ results, numerical differences are within 8% at $10^{-4} < x < 0.5$ and 24% at $x=0.8$ in the case $N_x=100$, within 3% at $10^{-4} < x < 0.5$ and 8% at $x=0.8$ in $N_x=300$, and within 0.7% at $10^{-4} < x < 0.5$ and 2% at $x=0.8$ in $N_x=1000$.

Evolution results of a gluon distribution are shown in Figs. 3a and 3b, and they show similar tendency to those in Figs. 2a and 2b. In Fig. 3a, N_t is varied with fixed $N_x=1000$. In comparison with the $N_t=1000$ results in Fig. 3a, numerical differences are within 5% at $10^{-4} < x < 0.6$ in the $N_t=20$ case, within 2% at $10^{-4} < x < 0.6$ in $N_t=50$, and within 0.4% at $10^{-4} < x < 0.6$ in $N_t=200$. In Fig. 3b, N_x is varied with fixed $N_t=200$. In comparison with the $N_x=4000$ results in Fig. 3b, numerical differences are within 25% at $10^{-4} < x < 0.6$ in the case $N_x=100$, within 8% at $10^{-4} < x < 0.6$ in $N_x=300$, and within 1% at $10^{-4} < x < 0.2$ and within 2% at $0.2 < x < 0.6$ in $N_x=1000$. The accuracy is slightly worse in the gluon distribution but it is mainly in the medium x region, which is not important in the gluon distribution.

From these results, we recommend to use $N_t \geq 200$ and $N_x \geq 1000$ in the singlet case for getting accuracy better than 1% at $0.0001 < x < 0.5$ and 2% at $0.5 < x < 0.8$ in the singlet-quark distribution, and accuracy is better than 1% at $0.0001 < x < 0.2$ and 2% at $0.2 < x < 0.6$ in the gluon distribution. Typical running time with $N_t=200$ and $N_x=1000$ on the AlphaServer is about one hour in the NLO singlet case.

We also check numerical accuracy of our evolution results in the case of $q_i + \bar{q}_i$

distributions, in the case with the recombinations, and in the case of nuclear parton distributions. However, the results have similar dependency on N_t and N_x , so that they are not discussed in this paper. A user can always check one's evolution results by changing N_t and N_x if one is suspicious about the accuracy.

The one-step evolution, e.g. $xq_s(x, Q_0^2) \rightarrow xq_s(x, Q^2)$, is used for getting the above results. We check the accuracy in the two-step evolution case, e.g. $xq_s(x, Q_0^2) \rightarrow xq_s(x, Q^2) \rightarrow xF_s(x, Q^2)$, by calculating the F_2 structure function of the proton with the MRS(G) input distributions. We find that the accuracy is better than 1% in the region ($10^{-4} < x < 0.8$) by taking $N_t=200$ and $N_x=1000$. Similar results are obtained in the recombination case, so that we do not discuss their numerical details.

From the above discussions, we had better use $N_t \geq 200$ and $N_x \geq 1000$ for getting accuracy better than 2%. Typical running time could be an hour on the AlphaServer. If the program is run on a SUN workstation, it could take a significant amount of running time. Therefore, a user may use a reasonably powerful machine in running the program BF1.

6.2 Comparisons with experimental data

We first compare nonsinglet evolution results with CDHSW F_3 -structure-function data [15] in neutrino reactions. We choose the initial distribution as the MRS(G) $xu_v + xd_v$ distribution at $Q_0^2=4 \text{ GeV}^2$ [10], $xu_v + xd_v = 2.704x^{0.593}(1-0.76\sqrt{x}+4.20x)(1-x)^{3.96} + 0.2513x^{0.335}(1+8.63\sqrt{x}+0.32x)(1-x)^{4.41}$. The two-step part of the evolution program is used for calculating $xF_3(x, Q^2)$ from the initial $xu_v(x, Q_0^2) + xd_v(x, Q_0^2)$. Chosen input parameters are the following in the NLO case: IOUT=2, INPUT=1, IREAD=1, MODIFY=1, INDIST=1, IORDER=2, ITYPE=3, ISTEP=2, IMORP=1, Q02=4.0, Q2=400.0, DLAM=0.255, NF=4, XX=0.045, NX=1000, NT=50, NSTEP=100, NXMIN=-4, NA=1, RFM=0.0, and DKHT=0.0. The LO evolution is also calculated by choosing IORDER=1. The results are shown in Fig. 4, in which the solid (dashed) curves indicates the NLO (LO) calculations at $x=0.045, 0.225$, and 0.55 . The LO results are different from the RK-MK-SK results in Ref. [6] because the initial distribution is different. The LO and NLO xF_3 are already different at the starting point ($Q^2=4 \text{ GeV}^2$) due to the NLO contributions from the coefficient function. The figure shows that the BF1 evolution agrees with the experimental Q^2 dependence. As it is obvious from the figure, the NLO contributions become significant at small Q^2 ($\approx 1 \text{ GeV}^2$).

Next, evolution of the proton F_2 structure function is studied. As it is shown in the previous subsection, the BF1 program can be run at small x , as small as $x = 10^{-4}$, with good accuracy, so that evolution results could be compared with recent HERA F_2 data. The initial distributions are the MRS(G) distributions at $Q_0^2=4 \text{ GeV}^2$. First, we calculate $F_{2,d^+}(x, Q^2)$ and $F_{2,S}(x, Q^2)$ by setting the initial ones as $QI0 = +0.2513x^{0.335}(1+8.63\sqrt{x}+0.32x)(1-x)^{4.41} + 0.4(1-0.02)1.74x^{-0.067}(1-3.45\sqrt{x}+10.3x)(1-x)^{10.1} + 0.043x^{0.3}(1-x)^{10.1}(1+64.9x)$, $xq_s = 2.704x^{0.593}(1-0.76\sqrt{x}+4.20x)(1-$

$x)^{3.96} + 0.2513x^{0.335}(1 + 8.63\sqrt{x} + 0.32x)(1 - x)^{4.41} + 1.74x^{-0.067}(1 - 3.45\sqrt{x} + 10.3x)(1 - x)^{10.1}$, and $xg = 1.51x^{-0.301}(1 - 4.14\sqrt{x} + 10.1x)(1 - x)^{6.06}$ with the input parameters: IOUT=6, INPUT=1, IREAD=1, MODIFY=1, INDIST=1, IORDER=2, ITYPE=2, ISTEP=2, IMORP=2, Q02=4.0, Q2=200.0, DLAM=0.255, NF=4, XX=0.0013, NX=1000, NT=200, NSTEP=100, NXMIN=-4, NA=1, RFM=0.0, and DKHT=0.0. The scale parameter is $\Lambda=0.255$ GeV and the number of flavor is four in the evolution. Next, $F_{2,s+}(x, Q^2)$ is calculated with $xs^+ = 0.2(1 - 0.02)1.74x^{-0.067}(1 - 3.45\sqrt{x} + 10.3x)(1 - x)^{10.1}$. These evolution results are added to give $F_2^p(x, Q^2) = -(1/3)[F_{2,d+}(x, Q^2) + F_{2,s+}(x, Q^2)] + (4/9)F_{2,s}(x, Q^2)$. The LO Altarelli-Parisi and Mueller-Qiu evolution results are also obtained by changing IORDER and MODIFY. These results are shown in Fig. 5 with various F_2^p data at $x \approx 0.0013, 0.013, 0.13$, and 0.45 from SLAC [16, 17] ($x=0.14, 0.45$), BCDMS [18] ($x=0.14, 0.45$), EMC [19, 17] ($x=0.125, 0.45$), NMC [20] ($x=0.0125, 0.14$), Fermilab-E665 [21] ($x=0.0012, 0.012$), ZEUS [22] ($x=0.0016, 0.014, 0.11$), and H1 [23] ($x=0.0013, 0.013, 0.13$). The solid, dashed, dot-dashed curves are obtained in the LO Altarelli-Parisi, NLO Altarelli-Parisi, and NLO Mueller-Qiu evolution equations respectively. The NLO Q^2 dependence agrees with the experimental data as shown in the figure, except for the Fermilab-E665 at small x and at small Q^2 where perturbative QCD would not work. At this stage, it seems that F_2^p data are not accurate enough to find the recombination effects on the evolution. We do not step into the details of recombination analysis in comparison with the HERA data.

Finally, Q^2 evolution of a nuclear structure function F_2^A is studied. Q^2 dependence of the ratio $R_2^{Ca} \equiv F_2^{Ca}/F_2^D$ had been measured by NMC [24]. We compare our evolution with the NMC data in Figs. 6a, 6b, 6c, and 6d at $x=0.0085, 0.035, 0.125$, and 0.45 . We assume that F_2^D is equal to the nucleon one for simplicity. The initial distributions at $Q_0^2=0.8$ GeV² in the nucleon are taken from Ref. [4]: $xq_{NS} = xu_v + xd_v = 1.967x^{0.501}(1 - x)^{3.89}(1 + 9.27x)$, $xq_S = 1.967x^{0.501}(1 - x)^{3.89}(1 + 9.27x) + 2.058x^{0.294}(1 - x)^{11.2}(1 + 7.95x)$, and $xg = 16.11x^{0.839}(1 - x)^{5.29}(1 - 0.597x)$. Those in the calcium nucleus are $xq_{NS}^{Ca} = 1.840x^{0.472}(1 - 0.984x)^{4.06}(1 + 9.33x)$, $xq_S^{Ca} = 1.840x^{0.472}(1 - 0.984x)^{4.06}(1 + 9.33x) + 6.423x^{0.600}(1 - x)^{8.13}(1 - 0.568x)$, and $xg^{Ca} = 179.2x^{1.95}(1 - x)^{7.32}(1 - 0.619x)$. Both nonsinglet and singlet structure functions are calculated. Then, we obtain $F_2^A = (1/18)F_{2,NS}^A + (2/9)F_{2,S}^A$ for isoscalar nucleus because $SU(3)_{flavor}$ symmetry is assumed in antiquark distributions in Ref. [4]. In Figs. 6a, 6b, 6c, and 6d, the solid, dashed, dot-dashed curves are obtained in the LO Altarelli-Parisi, NLO Altarelli-Parisi, and NLO Mueller-Qiu evolution equations respectively with $\Lambda=0.2$ GeV and $N_f=3$. As shown by the figures, NLO and recombination contributions to the ratio are conspicuous at small x ($=0.0085, 0.035$). They are very small at medium x ($=0.45$) in Fig. 6d; however, it does not mean that their contributions to the structure functions themselves are very small. If we evolve F_2 from $Q_0^2=0.8$ GeV², the recombination effects are larger than the NLO ones. It is interesting to find such large recombination contributions in Fig. 6a. However, the recombination cannot be tested at this stage because we do not have the data in the wide Q^2 region at small x .

7. Conclusions

We investigated numerical solution of Q^2 evolution equations of spin-independent parton distributions (and structure functions) in the nucleon and in nuclei by using the brute-force method. Two types of evolution equations are studied. One is the usual Altarelli-Parisi equations and the other is the modified ones due to parton recombinations (Mueller-Qiu).

We divide the variables x and t into small steps and simply solve the evolution equations. Numerical accuracy depends essentially on the numbers N_x and N_t . We obtain excellent numerical solution in the wide x range ($0.0001 \leq x \leq 0.8$) by taking large enough N_x and N_t . We recommend to use $N_x \geq 1000$ and $N_t \geq 50$ in the nonsinglet case and $N_x \geq 1000$ and $N_t \geq 200$ in the singlet for getting numerical accuracy better than 2% in the x range, $0.0001 < x < 0.8$.

We provide the FORTRAN program BF1, which can be run by supplying the input parameters and the input distribution(s). Parton distributions xq_{NS} , xq_S , $xq_i + x\bar{q}_i$ (corresponding structure functions), xg , and those in nuclei could be evolved in the program. The program can also handle the Q^2 devolution from Q_0^2 to smaller Q^2 . This is a very useful program in studying structure functions in the nucleon and in nuclei. Typical running CPU time is five minutes on the AlphaServer 2100 4/200 in the nonsinglet and one hour in the singlet. Therefore, a reasonably powerful machine should be used for running the BF1 program in the singlet case.

Acknowledgments

This research was partly supported by the Grant-in-Aid for Scientific Research from the Japanese Ministry of Education, Science, and Culture under the contract number 06640406 and also by the U.S. Department of Energy under the contract number DE-AC02-76CH00016. MM and SK thank the Research Center for Nuclear Physics in Osaka for making them use computer facilities. They thank W. Melnitchouk for communications on NLO effects in Ref. [25] and thank A. Brüll, E. Rondio, and H. M. Schellman for providing them experimental data. SK was supported by the Japan Society for Promotion of Science through the Japan/US cooperation program in the field of high-energy physics for his visiting Brookhaven National Laboratory (BNL). They would like to thank BNL for its hospitality during their stay.

Appendix A. Running coupling constants

Running coupling constant in the leading order (LO) is

$$\alpha_s^{LO}(Q^2) = \frac{4\pi}{\beta_0 \ln(Q^2/\Lambda^2)} \quad , \quad (A.1)$$

and the one in the next-to-leading order (NLO) is [26]

$$\alpha_s^{NLO}(Q^2) = \frac{4\pi}{\beta_0 \ln(Q^2/\Lambda^2)} \left[1 - \frac{\beta_1 \ln \ln(Q^2/\Lambda^2)}{\beta_0^2 \ln(Q^2/\Lambda^2)} \right] \quad . \quad (A.2)$$

In Eq. (A.2), the renormalization scheme is \overline{MS} and Λ is the QCD scale parameter in this scheme. β_0 and β_1 are given by

$$\beta_0 = \frac{11}{3}C_G - \frac{4}{3}T_R N_f \quad , \quad \beta_1 = \frac{34}{3}C_G^2 - \frac{10}{3}C_G N_f - 2C_F N_f \quad , \quad (A.3)$$

with the color constants

$$C_G = N_c \quad , \quad C_F = \frac{N_c^2 - 1}{2N_c} \quad , \quad T_R = \frac{1}{2} \quad . \quad (A.4)$$

N_c is the number of color ($N_c=3$) and N_f is the number of flavor.

Appendix B. Splitting functions

Splitting functions in the leading order are

$$\begin{aligned} P_{qq}^{(0)}(x) &= C_F \left[\frac{1+x^2}{(1-x)_+} + \frac{3}{2} \delta(1-x) \right] \quad , \\ P_{qg}^{(0)}(x) &= 2T_R \left[x^2 + (1-x)^2 \right] \quad , \\ P_{gq}^{(0)}(x) &= C_F \frac{1+(1-x)^2}{x} \quad , \\ P_{gg}^{(0)}(x) &= 2C_G \left[\frac{x}{(1-x)_+} + \frac{1-x}{x} + x(1-x) + \left(\frac{11}{12} - \frac{1}{3} \frac{N_f T_R}{C_G} \right) \delta(1-x) \right] \quad , \end{aligned} \quad (B.1)$$

where the $+$ function is defined by

$$\int_0^1 dx \frac{f(x)}{(1-x)_+} = \int_0^1 dx \frac{f(x) - f(1)}{1-x} \quad . \quad (B.2)$$

It should be noted that the above integration is defined in the region $0 \leq x \leq 1$.

The NLO splitting functions for $q_i^+(x)$ and $g(x)$ are given by Herrod and Wada [8, 9]

$$\begin{aligned}
P_{q_i^+ q_j^+}^{(1)}(x) &= \delta_{ij} P_{q^+, NS}^{(1)}(x) + 2C_F T_R F_{qq}(x) \quad , \\
P_{q_i^+ g}^{(1)}(x) &= -C_G T_R F_{qg}^1(x) - C_F T_R F_{qg}^2(x) \quad , \\
P_{gq_i^+}^{(1)}(x) &= -C_F^2 F_{gq}^1(x) - C_F C_G F_{gq}^2(x) - C_F T_R N_f F_{gq}^3(x) \quad , \\
P_{gg}^{(1)}(x) &= C_G T_R N_f F_{gg}^1(x) + C_F T_R N_f F_{gg}^2(x) + C_G^2 F_{gg}^3(x) \quad .
\end{aligned} \tag{B.3}$$

The NLO nonsinglet splitting function for a “ $q \pm \bar{q}$ type” distribution [$q_{NS} = \sum_i a_i(q_i \pm \bar{q}_i)$] is given by [8]

$$\begin{aligned}
P_{q^\pm, NS}^{(1)}(x) &= C_F^2 \left\{ P_F(x) \pm P_A(x) + \delta(1-x) \left[\frac{3}{8} - \frac{1}{2}\pi^2 + \zeta(3) - 8\tilde{S}(\infty) \right] \right\} \\
&+ \frac{1}{2} C_F C_A \left\{ P_G(x) \mp P_A(x) + \delta(1-x) \left[\frac{17}{12} + \frac{11}{9}\pi^2 - \zeta(3) + 8\tilde{S}(\infty) \right] \right\} \\
&+ C_F T_R N_f \left\{ P_{N_F}(x) - \delta(1-x) \left(\frac{1}{6} + \frac{2}{9}\pi^2 \right) \right\}
\end{aligned} \tag{B.4}$$

where $P_F(x)$, $P_G(x)$, $P_{N_F}(x)$, and $P_A(x)$ are given by Curci, Furmanski, and Petronzio [9] as

$$\begin{aligned}
P_F(x) &= -2 \frac{1+x^2}{1-x} \ln x \ln(1-x) - \left(\frac{3}{1-x} + 2x \right) \ln x - \frac{1}{2}(1+x) \ln^2 x - 5(1-x) \quad , \\
P_G(x) &= \frac{1+x^2}{(1-x)_+} \left[\ln^2 x + \frac{11}{3} \ln x + \frac{67}{9} - \frac{1}{3}\pi^2 \right] + 2(1+x) \ln x + \frac{40}{3}(1-x) \quad , \\
P_{N_F}(x) &= \frac{2}{3} \left[\frac{1+x^2}{(1-x)_+} \left(-\ln x - \frac{5}{3} \right) - 2(1-x) \right] \quad , \\
P_A(x) &= 2 \frac{1+x^2}{1+x} \int_{x/(1+x)}^{1/(1+x)} \frac{dz}{z} \ln \frac{1-z}{z} + 2(1+x) \ln x + 4(1-x) \quad .
\end{aligned} \tag{B.5}$$

The ζ function is defined by $\zeta(k) = \sum_{n=1}^{\infty} \frac{1}{n^k}$ and the numerical value ($\zeta(3)=1.2020569\dots$) is taken from Ref. [27]. $\tilde{S}(\infty)$ is given by the ζ function as $\tilde{S}(\infty) = -\frac{5}{8}\zeta(3)$. The integral in $P_A(x)$ is expressed in terms of the Spence function $S(x)$:

$$\int_{x/(1+x)}^{1/(1+x)} \frac{dz}{z} \ln \frac{1-z}{z} = S\left(\frac{x}{1+x}\right) - S\left(\frac{1}{1+x}\right) - \frac{1}{2} \left[\ln^2 \frac{1}{1+x} - \ln^2 \frac{x}{1+x} \right] \quad , \tag{B.6}$$

where $S(x)$ is defined by

$$S(x) = \int_x^1 dz \frac{\ln z}{1-z} \quad . \tag{B.7}$$

It should be noted that other convention is sometimes used, namely $-S(x)$ may be called the Spence function [27]. It is useful to use a series expansion form for numerical calculations [27]:

$$S(x) = - \sum_{k=1}^{\infty} \frac{(1-x)^k}{k^2} . \quad (B.8)$$

The functions F_{qq} , F_{qg} , F_{gq} , and F_{gg} in Eq. (B.3) are defined by

$$\begin{aligned} F_{qq}(x) &= \frac{20}{9} \frac{1}{x} - 2 + 6x - \frac{56}{9} x^2 + \left(1 + 5x + \frac{24}{9} x^2\right) \ln x - (1+x) \ln^2 x \quad , \\ F_{qg}^1(x) &= -\frac{40}{9} \frac{1}{x} + 4 - 50x + \frac{436}{9} x^2 - \left(2 + 16x + \frac{88}{3} x^2\right) \ln x \\ &\quad + (2+4x) \ln^2 x + 8x(1-x) \ln(1-x) \\ &\quad + \left(2-4x+4x^2\right) \left[\ln^2(1-x) - \frac{1}{6} \pi^2\right] - 4(1+2x+2x^2) J_x \quad , \\ F_{qg}^2(x) &= -14 + 29x - 20x^2 + (-3+4x-8x^2) \ln x \\ &\quad - (1-2x+4x^2) \ln^2 x - 8x(1-x) \ln(1-x) \\ &\quad + (2-4x+4x^2) \left[-\ln^2(1-x) + 2\ln x \ln(1-x) + \frac{1}{3} \pi^2\right] \quad , \\ F_{gq}^1(x) &= \frac{5}{2} + \frac{7}{2} x - \left(2 + \frac{7}{2} x\right) \ln x + \left(1 - \frac{1}{2} x\right) \ln^2 x \\ &\quad + \left(\frac{6}{x} - 6 + 5x\right) \ln(1-x) + \left(\frac{2}{x} - 2 + x\right) \ln^2(1-x) \quad , \\ F_{gq}^2(x) &= -\frac{1}{x} - \frac{19}{9} - \frac{37}{9} x - \frac{44}{9} x^2 + \left(12 + 5x + \frac{8}{3} x^2\right) \ln x \\ &\quad - (2+x) \ln^2 x - \frac{1}{3} \left(\frac{22}{x} - 22 + 17x\right) \ln(1-x) \\ &\quad - \left(\frac{2}{x} - 2 + x\right) \left[\ln^2(1-x) - 2\ln x \ln(1-x) - \frac{1}{6} \pi^2\right] \\ &\quad + \left(\frac{4}{x} + 4 + 2x\right) J_x \quad , \\ F_{gq}^3(x) &= \frac{40}{9} \frac{1}{x} - \frac{40}{9} + \frac{32}{9} x + \frac{4}{3} \left(\frac{2}{x} - 2 + x\right) \ln(1-x) \quad , \\ F_{gg}^1(x) &= -\frac{20}{9} \frac{1}{(1-x)_+} - \frac{2}{9} \left(\frac{23}{x} - 29 + 19x - 23x^2\right) \\ &\quad - \frac{4}{3} (1+x) \ln x - \frac{4}{3} \delta(1-x) \quad , \end{aligned}$$

$$\begin{aligned}
F_{gg}^2(x) &= \frac{4}{3x} - 16 + 8x + \frac{20}{3}x^2 - (6 + 10x) \ln x \\
&\quad - 2(1+x) \ln^2 x - \delta(1-x) \quad , \\
F_{gg}^3(x) &= \frac{67}{9} \frac{1}{(1-x)_+} - \frac{8}{9} - \frac{1}{18}x - \left(\frac{47}{6} - \frac{25}{6}x + \frac{44}{3}x^2 \right) \ln x \\
&\quad + \left(\frac{1}{1-x} + \frac{1}{1+x} + \frac{5}{4} + 6x - 2x^2 \right) \ln^2 x \\
&\quad + \left(-\frac{11}{2x} + \frac{7}{2} + \frac{13}{4}x \right) \ln(1-x) + \frac{1}{4} \left(-\frac{5}{x} + 5 + 2x \right) \ln^2(1-x) \\
&\quad - \left(\frac{4}{1-x} + \frac{4}{x} - 5 + 7x - 4x^2 \right) \ln x \ln(1-x) + (1+x) I_x \\
&\quad + 4 \left(\frac{1}{1+x} - \frac{1}{x} - 2 - x - x^2 \right) J_x - \frac{1}{3} \pi^2 \left(\frac{1}{(1-x)_+} + \frac{1}{x} - 1 + 2x - x^2 \right) \\
&\quad + \delta(1-x) \left[-4\tilde{S}(\infty) + \frac{1}{2} \zeta(3) + \frac{8}{3} \right] \quad .
\end{aligned} \tag{B.9}$$

where I_x is the Spence function [$I_x = S(x)$] and J_x is defined by

$$J_x = -\frac{1}{12} \pi^2 - \ln x \ln(1+x) + S(1+x) \quad . \tag{B.10}$$

In the one-step evolution equation in Eq. (2.14), the matrix \mathbf{E} is introduced. Each matrix element is given by

$$\begin{aligned}
E_{qq}(x) &= -E(\gamma_{gq} C^g) \quad , \\
E_{qg}(x) &= E(\gamma_{qq} C^g) - E(\gamma_{qg} C^q) - E(\gamma_{gg} C^g) \quad , \\
E_{gq}(x) &= E(\gamma_{gq} C^q) \quad , \\
E_{gg}(x) &= -E_{qq}(x) \quad .
\end{aligned} \tag{B.11}$$

where

$$\begin{aligned}
E(\gamma_{gq} C^g) / 2C_F T_R &= -\frac{2}{3x} + \frac{20}{3} - \frac{2x}{3} - \frac{16x^2}{3} + \left(1 + 5x - \frac{4}{3}x^2 \right) \ln x \\
&\quad + (1+x) \left(\ln^2 x - 2 \ln x \ln(1-x) + 2I_x \right) \\
&\quad + \left(-\frac{4}{3x} - 1 + x + \frac{4}{3}x^2 \right) \ln(1-x) \quad ,
\end{aligned}$$

$$\begin{aligned}
E(\gamma_{qq}C^g)/C_F T_R &= -7 + 10x - (1 - 16x + 32x^2) \ln x - (1 - 2x + 4x^2) \ln^2 x \\
&\quad + (6 - 12x + 16x^2) \ln x \ln(1 - x) \\
&\quad + (5 - 36x + 32x^2) \ln(1 - x) \\
&\quad - 4(1 - 2x + 2x^2) \left[\ln^2(1 - x) - \frac{\pi^2}{6} \right] - 2(1 - 2x + 4x^2) I_x \quad , \\
E(\gamma_{gg}C^g)/C_F T_R &= 5 - 12x + 16x^2 + (1 + 8x - 12x^2) \ln x \\
&\quad + (1 - 2x + 4x^2) [-\ln^2 x + 2 \ln x \ln(1 - x)] \\
&\quad + (7 - 16x + 12x^2) \ln(1 - x) \\
&\quad + (1 - 2x + 2x^2) \left[-2 \ln^2(1 - x) + \frac{2}{3} \pi^2 \right] + 2(1 - 2x) I_x \quad , \\
E(\gamma_{gq}C^g)/\frac{1}{2}C_F^2 &= 3 + 6x - 3x \ln x + (2 - x) \ln^2 x \\
&\quad + \left(\frac{12}{x} - 16 + 7x \right) \ln(1 - x) \\
&\quad + 2 \left(\frac{2}{x} - 2 + x \right) \left[-\ln^2(1 - x) + \frac{1}{3} \pi^2 \right] \\
&\quad - 2(2 - x) \ln x \ln(1 - x) + 2 \left(\frac{4}{x} - 2 + x \right) I_x \quad , \\
E(\gamma_{gg}C^g) &= C_G T_R A + \frac{4}{3} T_R^2 N_f B \quad .
\end{aligned} \tag{B.12}$$

A and B in the above equation are

$$\begin{aligned}
A &= -\frac{4}{3x} + 18 + \frac{154}{3}x - \frac{193}{3}x^2 + \left(\frac{17}{3} + \frac{170}{3}x - \frac{40}{3}x^2 \right) \ln x \\
&\quad + 2(1 + 4x) (\ln^2 x + 2I_x) - \left(\frac{8}{3x} + \frac{5}{3} + \frac{122}{3}x - \frac{136}{3}x^2 \right) \ln(1 - x) \\
&\quad - 4(1 - 2x + 2x^2) \left[\ln^2(1 - x) - \frac{\pi^2}{6} \right] - 8x(3 - x) \ln x \ln(1 - x) \quad , \\
B &= -1 + 8x - 8x^2 - (1 - 2x + 2x^2) \ln \left(\frac{x}{1 - x} \right) \quad .
\end{aligned} \tag{B.13}$$

In the above equation, we corrected the factor $(17/3 + 170x/3 - 40x^2/3)$, which was $(17 + 170x/3 - 40x^2/3)$ in the original paper [8].

The splitting function $\tilde{\bar{P}}_{gg} = x\bar{P}_{gg}$ is given by

$$\bar{P}_{gg}(x) = 2(-2x + 15x^2 - 30x^3 + 18x^4) \quad . \tag{B.14}$$

Appendix C. Coefficient functions

The coefficient functions $C_n^{q,g}(x, \alpha_s)$ in Eqs. (2.10) and (2.11) are written by the functions $B_n^{q,g}(x)$:

$$C_n^q(x, \alpha_s) = \delta(1-x) + \frac{\alpha_s}{4\pi} B_n^q(x) \quad , \quad C_n^g(x, \alpha_s) = \frac{\alpha_s}{4\pi} B_n^g(x) \quad . \quad (C.1)$$

The quark part is given by [8]

$$\begin{aligned} B_1^q(x) &= \frac{C_F}{2} [F_q(x) - 4x] \quad , \\ B_2^q(x) &= C_F F_q(x) \quad , \\ B_3^q(x) &= C_F [F_q(x) - 2 - 2x] \quad , \end{aligned} \quad (C.2)$$

where the function $F_q(x)$ is given by

$$F_q(x) = -\frac{3}{2} \frac{1+x^2}{(1-x)_+} + \frac{1}{2} (9+5x) - 2 \frac{1+x^2}{1-x} \ln x + 2(1+x^2) \left[\frac{\ln(1-x)}{1-x} \right]_+ - \delta(1-x) \left(9 + \frac{2}{3} \pi^2 \right) . \quad (C.3)$$

The gluon part is:

$$\begin{aligned} B_1^g(x) &= 2T_R [F_g(x) - 4x(1-x)] \quad , \\ B_2^g(x) &= 4T_R F_g(x) \quad , \end{aligned} \quad (C.4)$$

where

$$F_g(x) = (1-2x+2x^2) \ln\left(\frac{1-x}{x}\right) + 8x(1-x) - 1 \quad . \quad (C.5)$$

References

- [1] V. N. Gribov and L. N. Lipatov, Sov. J. Nucl. Phys. 15 (1972) 438 and 675; G. Altarelli and G. Parisi, Nucl. Phys. B 126 (1977) 298; Yu. L. Dokshitzer, Sov. Phys. JETP 46 (1977) 641.
- [2] A. H. Mueller and J. Qiu, Nucl. Phys. B 268 (1986) 427; J. Qiu, Nucl. Phys. B 291 (1987) 746;
- [3] K. Golec-Biernat, M. W. Krasny, and S. Riess, Phys. Lett. B 337 (1994) 367.
- [4] S. Kumano, Phys. Rev. C48 (1993) 2016; C50 (1994) 1247; Phys. Lett. B 298 (1993) 171; B 342 (1995) 339; R. Kobayashi, S. Kumano, and M. Miyama, Phys. Lett. B 354 (1995) 465.
- [5] References to various methods are listed in the RK, MK, and SK paper in Ref. [6].
- [6] W. Furmanski and R. Petronzio, Nucl. Phys. B 195 (1982) 237; G. P. Ramsey, J. Comput. Phys. 60 (1985) 97; J. Blümlein, G. Ingelman, M. Klein, and R. Rückl, Z. Phys. C 45 (1990) 501; S. Kumano and J. T. Londergan, Comput. Phys. Commun. 69 (1992) 373; R. Kobayashi, M. Konuma, and S. Kumano, Comput. Phys. Commun. 86 (1995) 264; R. Kobayashi, M. Konuma, S. Kumano, and M. Miyama, Prog. Theo. Phys. Supplement, 120 (1995) in press; the singlet part is in progress.
- [7] N. Cabibbo and R. Petronzio, Nucl. Phys. B 137 (1978) 395; G. P. Ramsey, Ph. D. thesis, Illinois Institute of Technology (1982); W.-K. Tung, private communication (1991).
- [8] R. T. Herrod and S. Wada, Phys. Lett. B 96 (1980) 195; R. T. Herrod, S. Wada, B. R. Webber, Z. Phys. C 9 (1981) 351.
- [9] There are other publications on the NLO Altarelli-Parisi equations, G. Curci, W. Furmanski, and R. Petronzio, Nucl. Phys. B 175 (1980) 27; E. G. Floratos, R. Lacaze and C. Kounnas, Phys. Lett. B 98 (1981) 89 & 285; Nucl. Phys. B 192 (1981) 417.
- [10] A. D. Martin, W. J. Stirling, and R. G. Roberts, Phys. Lett. B 354 (1995) 155.
- [11] G. E. Forsythe, M. A. Malcolm, and C. B. Moler, *Computer Methods for Mathematical Computations* (Prentice-Hall, 1977).
- [12] E. G. Floratos, D. A. Ross, and C. T. Sachrajda, Nucl. Phys. B 129 (1977) 66 & B 152 (1979) 493.
- [13] W. A. Bardeen, A. J. Buras, D. W. Duke, and T. Muta, Phys. Rev. D 18 (1978) 3998.

- [14] P. N. Harriman, A. D. Martin, W. J. Stirling, and R. G. Roberts, Phys. Rev. D 42 (1990) 798; We use the HMRS program supplied by W. J. Stirling for testing the BF1 program.
- [15] P. Berge et al. (CDHSW collaboration), Z. Phys. C 49, (1991) 187; see also W. C. Leung et al. (CCFR collaboration), Phys. Lett. B 317 (1993) 655; A. L. Kataev and A. V. Sidorov, Phys. Lett. B 331 (1994) 179.
- [16] SLAC data in the report SLAC-PEP-357 are taken from [17].
- [17] R. G. Roberts and M. R. Whalley, J. Phys. G 17 (1991) D1.
- [18] A. C. Benvenuti et al. (BCDMS collaboration), Phys. Lett. B 223 (1989) 485.
- [19] J. J. Aubert et al. (EMC collaboration), Nucl. Phys. B 259 (1985) 189; Numerical data in the EMC report, CERN-PPE-90-175, are taken from Ref. [17] and they are used in our analysis.
- [20] P. Bjorkholm (NMC collaboration), Ph.D. thesis, Acta Universitatis Upsaliensis, Uppsala (1995).
- [21] A. V. Kotwal (Fermilab-E665 collaboration), report FERMILAB-CONF-95-046-E.
- [22] M. Derrick et al. (ZEUS collaboration), Z. Phys. C 65 (1995) 379.
- [23] T. Ahmed et al. (H1 collaboration), Nucl. Phys. B 439 (1995) 471.
- [24] P. Amaudruz et al. (NMC collaboration), Nucl. Phys. B 441 (1995) 3.
- [25] W. Melnitchouk, T. Weigl, and W. Weise, research in progress.
- [26] R. G. Roberts, *The Structure of the Proton* (Cambridge University Press, Cambridge, 1990).
- [27] M. Abramowitz and I. A. Stegun, *Handbook of Mathematical Functions* (Dover Publications, New York, 1972)

Figure Captions

Fig. 1 (a) N_t dependence of nonsinglet evolution results is shown. Next-to-leading-order Altarelli-Parisi evolution results are calculated by running the program BF1. $N_x=1000$ is fixed and N_t is varied ($N_t=10, 20$, and 500) in order to check numerical accuracy due to the choice of N_t . The initial distribution is the HMRS-B $xu_v + xd_v$ distribution at $Q_0^2=4 \text{ GeV}^2$. There are dotted, dashed, and solid curves at $Q^2=200 \text{ GeV}^2$ for $N_t=10, 20$, and 500 respectively; however, they cannot be distinguished in the figure because differences among them are fairly small. See text for the details of the input parameters. (b) N_x dependence is shown by taking fixed $N_t=50$. The dotted, dashed, dot-dashed, and solid curves are the results for $N_x=100, 300, 1000$, and 4000 respectively.

Fig. 2 (a) N_t dependence of singlet-quark evolution results is shown. Next-to-leading-order Altarelli-Parisi evolution results are calculated. $N_x=1000$ is fixed and N_t is varied. The initial distributions are the HMRS-B xq_s and xg distributions at $Q_0^2=4 \text{ GeV}^2$. The dotted, dashed, dot-dashed, and solid curves at $Q^2=200 \text{ GeV}^2$ for $N_t=20, 50, 200$, and 500 respectively. (b) N_x dependence is shown by taking fixed $N_t=200$. The dotted, dashed, dot-dashed, and solid curves are the results for $N_x=100, 300, 1000$, and 4000 respectively.

Fig. 3 (a) N_t dependence of gluon evolution results is shown. N_x is fixed at $N_x=1000$. The input parameters and the input distributions are the same with those in Fig. 2. The dotted, dashed, dot-dashed, and solid curves at $Q^2=200 \text{ GeV}^2$ are for $N_t=20, 50, 200$, and 500 . (b) N_x dependence is shown by taking fixed $N_t=200$. The dotted, dashed, dot-dashed, and solid curves are the results for $N_x=100, 300, 1000$, and 4000 respectively.

Fig. 4 Nonsinglet Q^2 evolution results are compared with CDHSW data. The initial distribution is the MRS(G) $xu_v + xd_v$ at $Q_0^2=4 \text{ GeV}^2$. The solid and dashed curves are the NLO and LO results at $x=0.045, 0.225$, and 0.55 .

Fig. 5 Q^2 evolution results of the proton's F_2 structure function at $x=0.0013, 0.013, 0.13$, and 0.45 are compared with various data in SLAC, BCDMS, EMC, NMC, Fermilab-E665, ZEUS, and H1 experiments. The solid, dotted, and dashed curves are obtained by using the NLO Altarelli-Parisi, LO Altarelli-Parisi, and NLO Mueller-Qiu equations respectively. F_2^p at $x=0.0013, 0.013$, and 0.13 are shown by $10 \cdot F_2^p(x=0.0013)$, $10^{2/3} \cdot F_2^p(x=0.013)$, and $10^{1/3} \cdot F_2^p(x=0.13)$.

Fig. 6 Q^2 dependence of the structure function ratio $F_2^{Ca}(x, Q^2)/F_2^D(x, Q^2)$ is calculated and results are compared with NMC data. The solid, dotted, and dashed curves are obtained by using the NLO Altarelli-Parisi, LO Altarelli-Parisi, and NLO Mueller-Qiu equations ($\Lambda=0.2 \text{ GeV}$, $N_f=3$) respectively at (a) $x=0.0085$, (b) 0.035 , (c) 0.125 , and (d) 0.45 . The input distributions in the nucleon and in

the calcium nucleus are taken from Ref. [4]. For example, AP (NLO) means that the next-to-leading-order Altarelli-Parisi equations are used in evolving F_2 in the nucleon and the one in the calcium, then the ratios are taken.

TEST RUN OUTPUT

IOUT= 3 INPUT= 1 IREAD= 1 MODIFY= 1 INDIST= 1
IORDER= 2 ITYPE= 4 ISTEP= 1 IMORP= 2
Q02= 4.0000 Q2= 200.000 DLAM= 0.2550 NF= 4
XX= 0.0000000 NX=1000 NT= 200 NSTEP= 50 NXMIN= -4
NA= 1 RFM= 0.00 DKHT= 0.000

0.000100	18.335139	66.652696
0.000120	17.128091	61.663113
0.000145	15.996575	57.000809
0.000174	14.936139	52.646335
0.000209	13.942574	48.581338
0.000251	13.011907	44.788502
0.000302	12.140385	41.251490
0.000363	11.324464	37.954894
0.000437	10.560801	34.884181
0.000525	9.846243	32.025646
0.000631	9.177817	29.366368
0.000759	8.552722	26.894167
0.000912	7.968325	24.597561
0.001096	7.422150	22.465735
0.001318	6.911875	20.488499
0.001585	6.435325	18.656257
0.001905	5.990469	16.959975
0.002291	5.575416	15.391153
0.002754	5.188411	13.941795
0.003311	4.827834	12.604385
0.003981	4.492194	11.371860
0.004786	4.180129	10.237586
0.005754	3.890402	9.195334
0.006918	3.621892	8.239259
0.008318	3.373589	7.363868
0.010000	3.144582	6.564002
0.012023	2.934037	5.834797
0.014454	2.741170	5.171655
0.017378	2.565211	4.570205
0.020893	2.405346	4.026253
0.025119	2.260649	3.535733
0.030200	2.129987	3.094648
0.036308	2.011924	2.699013

0.043652	1.904595	2.344797
0.052481	1.805604	2.027887
0.063096	1.711949	1.744079
0.075858	1.620025	1.489125
0.091201	1.525750	1.258859
0.109648	1.424866	1.049428
0.131826	1.313447	0.857641
0.158489	1.188551	0.681417
0.190546	1.048903	0.520250
0.229087	0.895387	0.375536
0.275423	0.731157	0.250490
0.331131	0.561477	0.149345
0.398107	0.393883	0.075655
0.478630	0.239332	0.029963
0.575440	0.113441	0.007968
0.691831	0.033130	0.001021
0.831764	0.002843	0.000023
1.000000	0.000000	0.000000

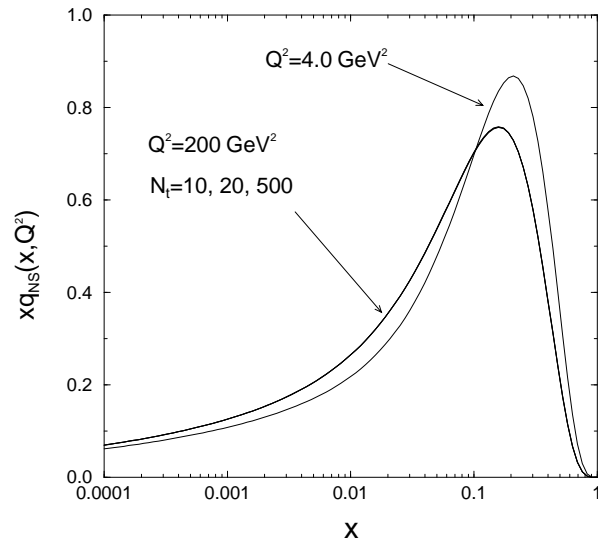


Figure 1 (a)

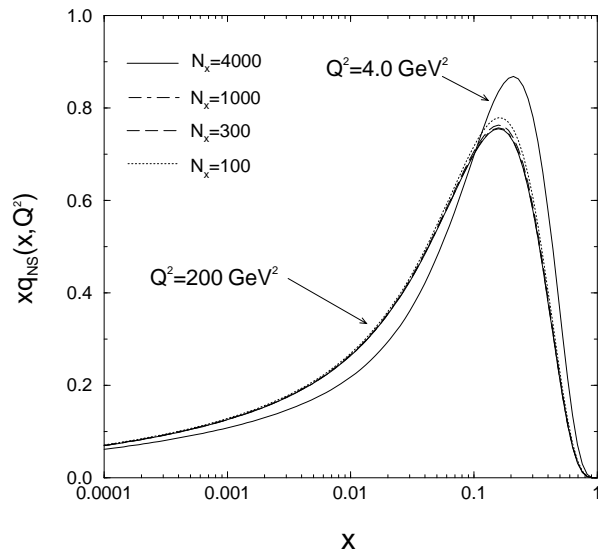


Figure 1 (b)

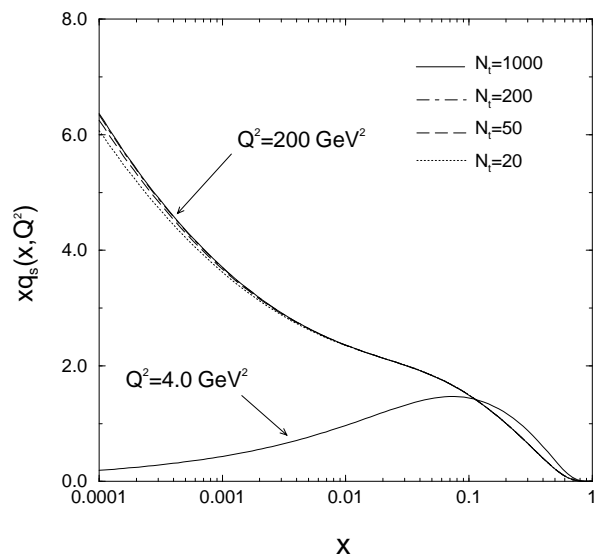


Figure 2 (a)

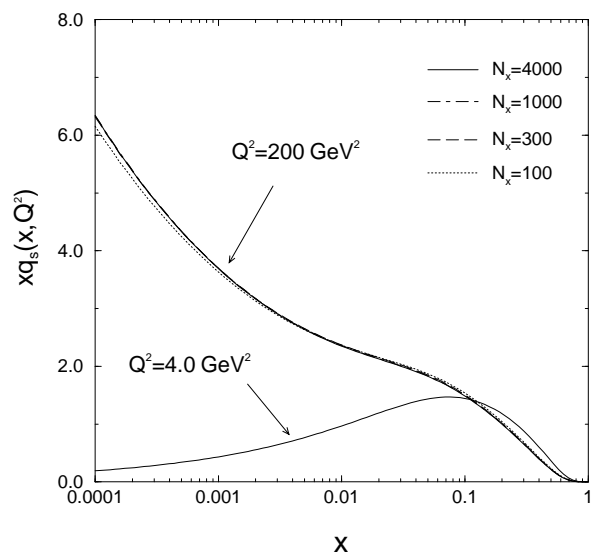


Figure 2 (b)

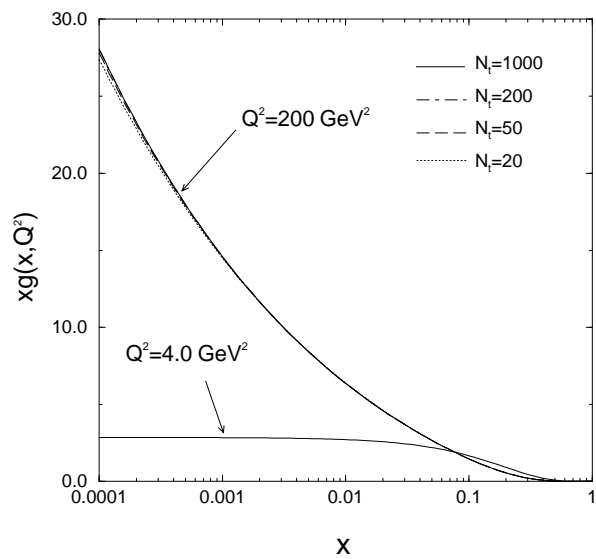


Figure 3 (a)

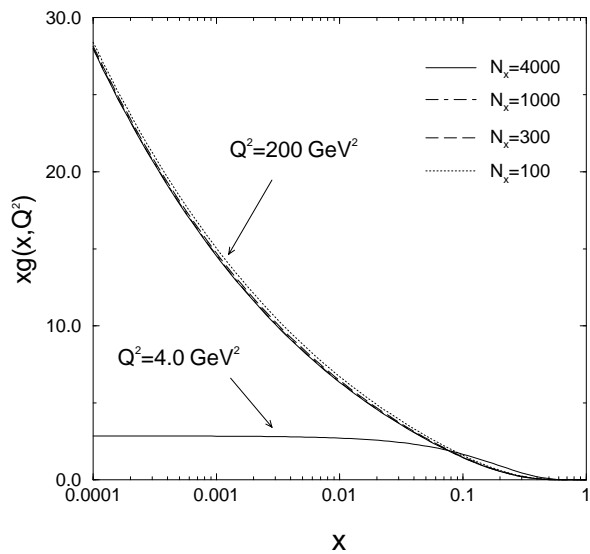


Figure 3 (b)

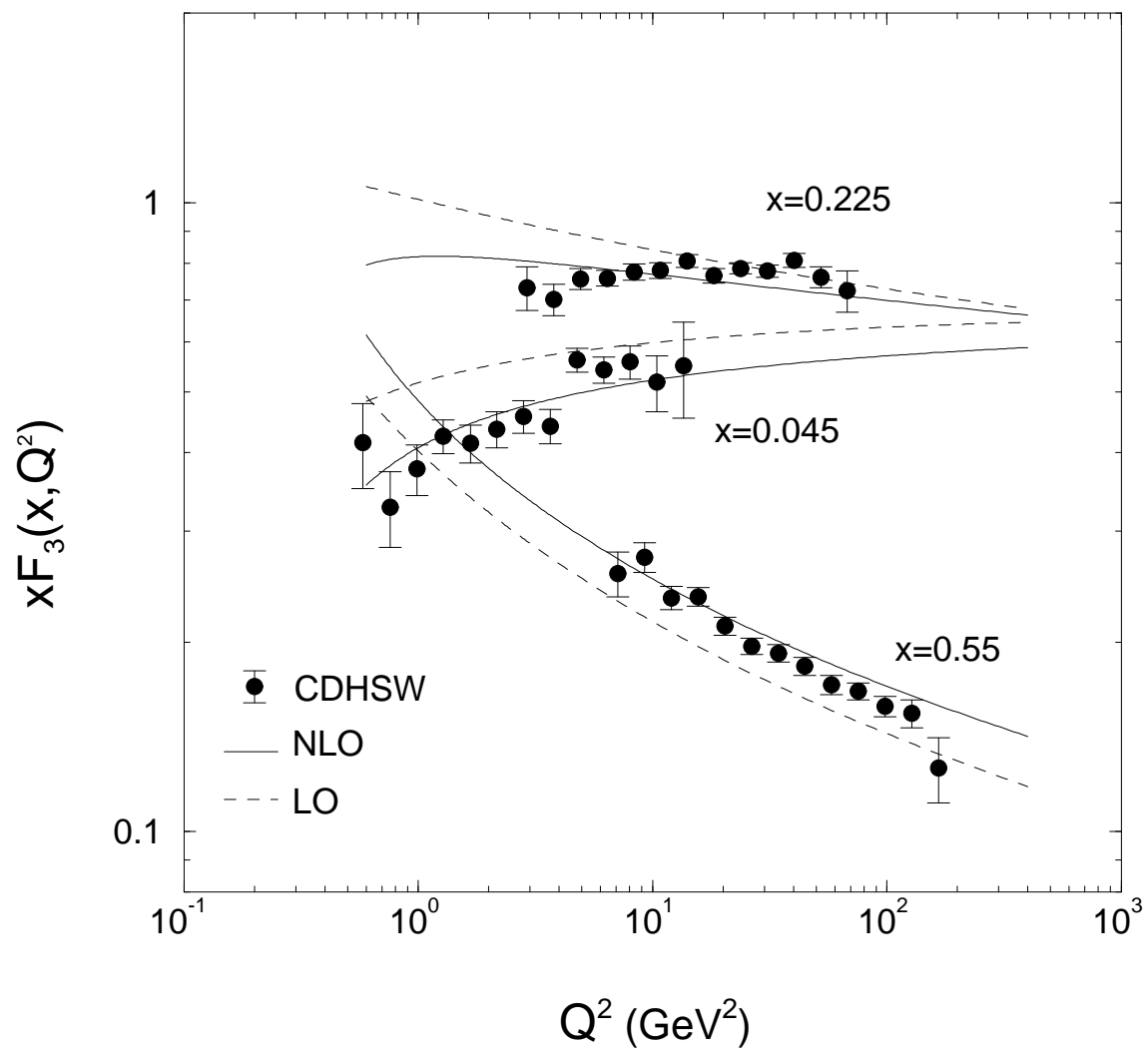


Figure 4

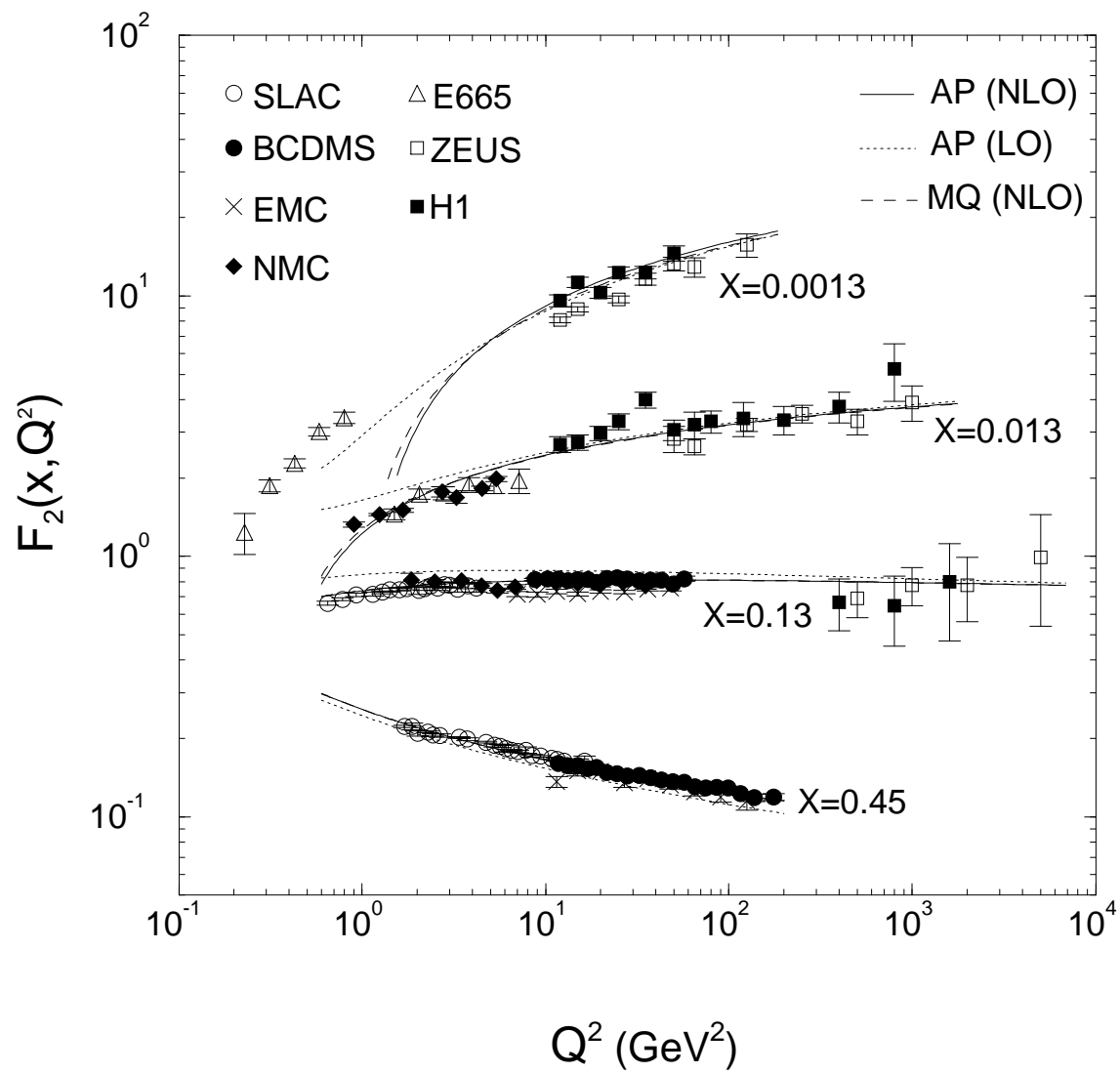


Figure 5

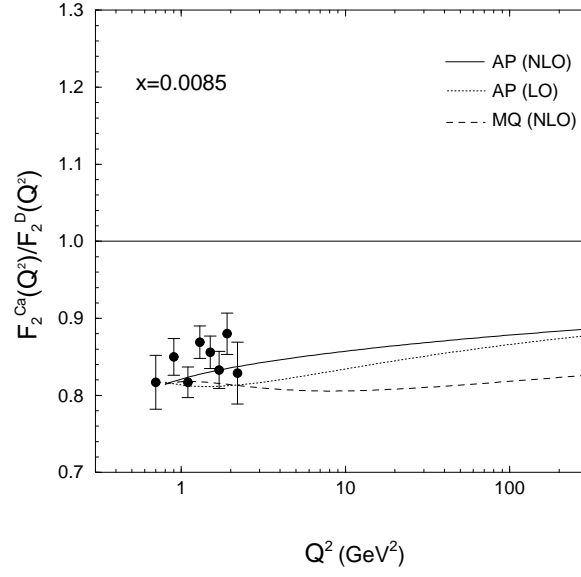


Figure 6 (a)

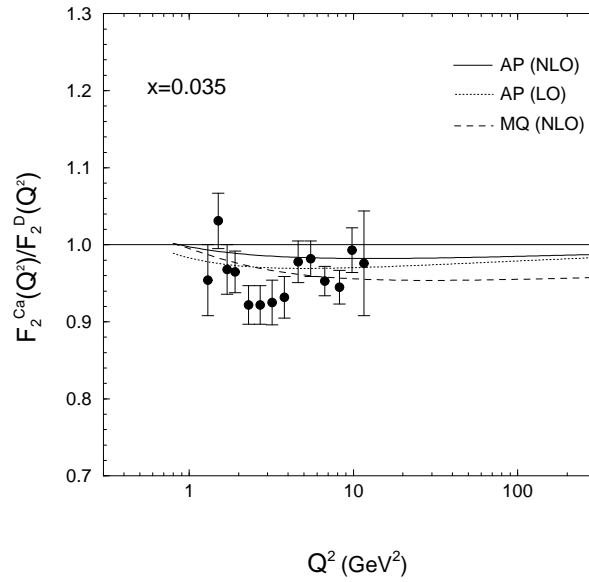


Figure 6 (b)

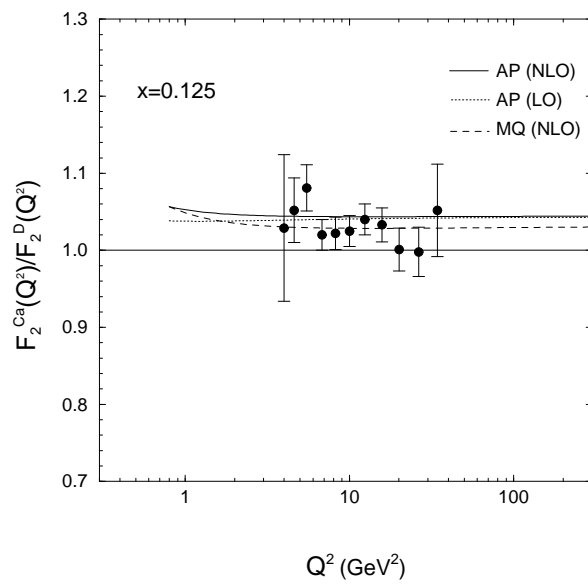


Figure 6 (c)

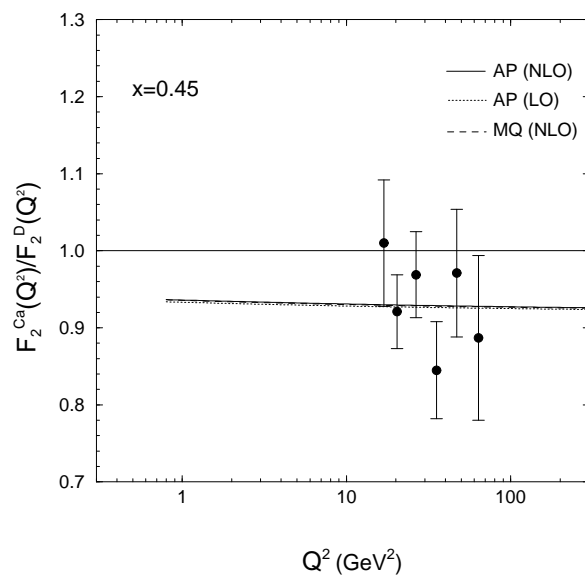


Figure 6 (d)